Rapid, large-scale species discovery in hyperdiverse taxa using 1D MinION sequencing

Amrita Srivathsan[1], Emily Hartop[2,5,6], Jayanthi Puniamoorthy[1], Wan Ting Lee[1], Sujatha Narayanan Kutty[1,4], Olavi Kurina[3], Rudolf Meier[1,4*]

[1] Department of Biological Sciences, National University of Singapore, 14 Science Drive 4

[2] Zoology Department, Stockholms Universitet, Stockholm, Sweden

[3] Estonian University of Life Sciences, Kreutzwaldi 5D, Tartu, Estonia

[4] Tropical Marine Science Institute, National University of Singapore, Singapore

[5] Station Linné, Öland, Sweden

[6] Naturhistoriska Riksmuseet, Stockholm, Sweden

*__Corresponding author__: Rudolf Meier: meier@nus.edu.sg

Keywords: NGS barcoding, DNA barcoding, Nanopore sequencing, MinION, large-scale species discovery

ABSTRACT

Background:

More than 80% of all animal species remain unknown to science. Most of these species live in the tropics and belong to animal taxa that combine small body size with high specimen abundance and large species richness. For such clades, using morphology for species discovery is slow because large numbers of specimens must be sorted using detailed microscopic investigations. Fortunately, species discovery could be greatly accelerated if DNA sequences could be used for sorting specimens to species. Morphological verification of such "molecular Operational Taxonomic Units" (mOTUs) could then be based on dissection of a small subset of specimens. However, this approach requires cost-effective and low-tech DNA barcoding techniques because well equipped, well-funded molecular laboratories are not readily available in many biodiverse countries.

Results:

We here document how MinION sequencing can be used for large-scale species discovery in a specimen- and species-rich taxon like the hyper-diverse fly family Phoridae (Diptera). We sequenced 7,059 specimens collected in a single Malaise trap in Kibale National Park, Uganda over the short period of eight weeks. We discovered >650 species which exceeded the number of phorid species currently described for the entire Afrotropical region. The barcodes were obtained using an improved low-cost MinION pipeline that increased the barcoding capacity sevenfold from 500 to 3,500 barcodes per flowcell. This was achieved by adopting 1D sequencing, re-sequencing weak amplicons on a used flowcell, and improving demultiplexing. Comparison with Illumina data revealed that the MinION barcodes were very accurate (99.99% accuracy, 0.46% Ns) and thus yielded very similar species units (match ratio: 0.991). Morphological examination of 100 mOTUs also confirmed good congruence with morphology (93% of mOTUs; >99% of specimens) and revealed that 90% of the putative species belong to

a neglected, megadiverse genus (*Megaselia*). We demonstrate for one *Megaselia* species how the molecular data can guide the description of a new species (*Megaselia sepsioides* sp. nov.).

Conclusions

We document that one field site in Africa can be home to an estimated 1000 species of phorids and speculate that the Afrotropical diversity could exceed 100,000 species. We furthermore conclude that low-cost MinION sequencers are very suitable for reliable, rapid, and large-scale species discovery in hyperdiverse taxa. MinION sequencing could quickly reveal the extent of the unknown diversity and is especially suitable for biodiverse countries with limited access to capital-intensive sequencing facilities.

INTRODUCTION

In 2011 the former president of the Royal Society, Robert May, wrote that "[w]e are astonishingly ignorant about how many species are alive on earth today, and even more ignorant about how many we can lose [and] yet still maintain ecosystem services that humanity ultimately depends upon." [1] Little has changed since 2011 and >80% of all extant animal species remain unknown to science [2]. Most of these unknown species belong to hyper-diverse and species-rich invertebrate clades. They are ubiquitous, contain most of the multicellular animal species, and often occur in great abundance. However, research on the species diversity of such clades is underdeveloped because it requires the examination of large numbers of specimens. These specimens have to be grouped into species before they can be either identified (if they belong to a known species) or described (if they are unknown to science).

In invertebrates, species discovery often starts with obtaining specimens via bulk sampling methods. In insects, one of the most widely used methods is Malaise trapping. Such traps routinely collect thousands, or even tens of thousands, of specimens per site and week; i.e., sorting all specimens to species-level virtually never happens and the world's natural history museums store billions of unsorted specimens. Species-level sorting is usually restricted to a few taxa with small to moderate numbers of specimens. It is accomplished in two stages. The first is grouping specimens into easily identifiable major taxa (e.g., major groups of beetles, flies, wasps). This type of pre-sorting is usually accomplished by parataxonomists with basic training in morphology (e.g., students). The main challenge is the second sorting stage; i.e., sorting to species-level. This work is best carried out by taxonomic experts whose techniques are, however, mostly effective for taxa that have fairly small numbers of specimens and species. In contrast, large, hyperdiverse and abundant taxa are ill-suited because they require dissection and microscopic study of many specimens. An alternative to species-level sorting by taxonomists is a hybrid approach that combines rapid pre-sorting to "morpho-species" by

61 parataxonomists with subsequent verification of morpho-species via DNA barcodes that are
62 obtained for a few specimens for each morpho-species [3]. DNA barcodes are only obtained for
63 few specimens because it would be too time-consuming and expensive to generate them for all
64 specimens using the traditional DNA barcoding methods that require formal DNA extractions
65 and Sanger sequencing [4]. Unfortunately, this widely used hybrid approach has three
66 problems. Firstly, species-level sorting by parataxonomists is very imprecise [5,6]. Secondly,
67 small-scale DNA barcoding tends to overlook morphologically cryptic species. Thirdly, the hybrid
68 approach requires a lot of manpower for morpho-species sorting.
69
70 An alternative approach to species discovery is the 'reverse workflow' of Wang et al. (2018) [4].
71 Here, every specimen in a sample is DNA barcoded with minimal or no damage to the specimen
72 [4, 7, 8] using simplified DNA extraction protocols and Illumina sequencing [9]. After barcoding,
73 the specimens are grouped into molecular Operational Taxonomic Units (mOTUs) that in most
74 cases represent species. The confirmation of these mOTUs as species comes last. Taxonomic
75 experts use morphology to study a subset of the specimens that were pre-sorted to putative
76 species based on DNA sequences. The selection of the specimens can be guided by the
77 genetic distance between individuals [3]. This "reverse workflow" has the advantage that
78 species-level sorting relies on DNA sequencing which can potentially be automated. It also
79 associates morphologically dissimilar males, females, and immature specimens that belong to
80 the same species [7]. However, barcoding all specimens in a sample is unrealistically expensive
81 with traditional Sanger sequencing. The implementation of the reverse workflow thus requires
82 more cost-effective sequencing solutions that are now provided by High Throughput
83 Sequencing platforms (e.g., Illumina, Nanopore, PacBio: [4, 8, 10-13]). For example, tens of
84 thousands of specimens can be barcoded on a single lane of Illumina HiSeq with the total cost
85 of a barcode being as low as 0.17 USD (including PCR cost, see discussion in Wang et al.,
86 2018 [4]). However, due to read length restrictions, barcodes obtained with Illumina are <400 bp

87 and new solutions for obtaining full-length barcodes based on PacBio [10] or MinION [14]
88 sequencing have only recently emerged.
89
90 Unfortunately, barcoding with Illumina and PacBio sequencing has some downsides. Firstly,
91 both technologies are only cost-effective if >10,000 specimens are simultaneously barcoded
92 because the cost of flowcells is high. Secondly, sequencing must usually be outsourced; i.e.,
93 amplicon pools have to be shipped to sequencing facilities. This is not a major concern in
94 developed countries, but it is often a problem for species discovery research in countries that
95 lack capital-intensive, high-throughput sequencing facilities or have restrictive regulations with
96 regard to the export of genetic material. It would thus be desirable to have alternative
97 sequencing techniques that are fast, scalable, cost-effective, and require low initial investment.
98 Such solutions would be particularly useful if barcoding could be accomplished under field
99 conditions and/or by citizen scientists [15-18].
100
101 Oxford Nanopore's MinION has the potential to be such a solution. It is a low-cost, portable
102 device and delivers real-time sequencing. However, it unfortunately still generates error-prone
103 data (ca. 10-15% [19]) at a fairly high cost per base pair. Therefore, its use and reliability for
104 large-scale specimen barcoding remains poorly explored. A first step toward the use of MinION
105 for barcoding was the recent demonstration that 500 DNA barcodes can be obtained on one
106 flowcell of MinION using $1D^2$ sequencing [14]. The study increased the throughput of one
107 MinION flowcell by one order of magnitude compared to existing protocols. However, the scale
108 was arguably still not sufficient for large-scale species discovery where thousands of specimens
109 have to be barcoded. Furthermore, the experiment used $1D^2$ sequencing, which requires
110 complicated and time-consuming library preparation techniques and access to computer servers
111 for base-calling. Here, we test whether the more straightforward, but less accurate, 1D
112 sequencing can be used for large-scale species discovery.

Improved species discovery techniques are particularly needed for hyperdiverse clades of invertebrates that have many species in the tropics. A good example are insects whose diversity is concentrated in four hyper-diverse insect orders: Coleoptera (beetles), Diptera (midges and flies), Hymenoptera (bees, wasps, and ants), and Lepidoptera (moths and butterflies). Species estimates for all Insecta vary between 3 and 13 million (reviewed by Stork, 2018 [20]) with only ca. 1,000,000 currently described [21]. Historically, Coleoptera has been considered the most species-rich order of insects which is said to have led the evolutionary biologist J. B. S. Haldane to remark that the creator must have had an “inordinate fondness for beetles.” [22]. However, it now appears that the impression that Coleoptera is the most species-rich order may have been due to an inordinate fondness of taxonomists for beetles. Recent studies suggest that Diptera and Hymenoptera may be more species-rich. For example, Forbes et al. [23] proposed that Hymenoptera contained more species than either Diptera or Coleoptera based on parasite host ratios for Microhymenoptera. Similarly, a large barcoding study of Canadian insects found that Hymenoptera and Diptera together accounted for two thirds of the 46,937 molecular Operational Units found (in the form of BINs or Barcode Index Numbers [24]). The study predicted that one dipteran family alone, gall midges (Cecidomyiidae), may have 16,000 species in Canada. Once extrapolated to a worldwide scale, the authors estimated that 1.8 million of the 10 million predicted insect species could be cecidomyiids [25]; i.e., a single family of Diptera would far surpass the number of described beetle species. Other studies similarly hint at the extraordinary richness of Diptera. For example, the Zurqui All Diptera Biodiversity Inventory (ZADBI) of a single site in Costa Rica was heavily reliant on specimens collected with two Malaise traps over one year [26]. Only 41,001 specimens (a small fraction of the hundreds of thousands collected) were studied by taxonomic experts [27]. These specimens belonged to 4,332 species of Diptera, of which 800 were Cecidomyiidae and 404 Phoridae [27], the fly family of focus here.

139 Phoridae, or scuttle flies, is a family of true flies with approximately 4,300 described species
140 [28]. Currently, only 466 species of phorids have been described for the Afrotropical Region [28]
141 while Henry Disney, a world expert on the family, has recorded 75 species of phorids in his
142 suburban garden in Cambridge alone [29]. Similarly, the BioSCAN project in Los Angeles
143 recorded up to 82 species in city backyards [29]. These numbers make it very likely that the
144 Afrotropical fauna is very large and currently vastly understudied. But not all phorid taxa are
145 equally poorly sampled. The main obstacle to understanding phorid diversity is *Megaselia*
146 Rondani which contains >1,600 of the 4,300 described species. This makes *Megaselia* "one of
147 the largest, most biologically diverse and taxonomically difficult genera in the entire animal
148 kingdom" [30]. In groups like *Megaselia*, the obstacles to completing species discovery with
149 traditional methods appear insurmountable. Extremely large numbers of specimens are
150 routinely collected which can belong to very large numbers of species. This makes sorting such
151 samples into species-level units using traditional workflows very labour-intensive. Rare and new
152 species are often hidden among very large numbers of common and described species. The
153 rare species cannot be found without the microscopic study of thousands of specimens for
154 which prodigious notes have to be taken. Detailed drawings must be prepared (for *Megaselia*
155 drawings of male genitalia are essential) – often based on dissections and slide mounts. This
156 traditional workflow thus discourages all but the most tenacious taxonomists from taking up the
157 study of hyper-diverse genera within insects.
158
159 Here, we test whether 1D MinION sequencing can help to reveal phorid diversity more
160 comprehensively by relegating the sorting to species level to sequencing. MinION sequencing is
161 here applied to ca. 30% of the phorid specimens that were collected in a single Malaise trap in
162 Kibale National Park, Uganda. We describe how we processed ~8,700 specimens, obtained
163 ~7,000 accurate barcodes, and found >650 putative species. All this was accomplished using a
164 workflow that would take less than a month.

165

166

167 **RESULTS**

168 **1. MinION based DNA barcoding**

169 The experiment was designed to obtain full-length COI barcodes via tagged amplicon
170 sequencing for two sets of specimens. A total of 8,699 phorid flies were processed (Set 1:
171 4,275; Set 2: 4,519; 95 specimens were duplicated in both sets) (Fig. 1). In order to assess
172 amplification success rates, a subset of PCR products for each of the ninety-two 96-well plates
173 were verified with agarose gels. Amplification success rates were estimated to be 86% and 74%
174 for the two sets of specimens (80.7% overall); i.e., we estimated that >3,600 and >3,300 DNA
175 barcodes should be obtainable via MinION sequencing given that gels tend to underestimate
176 amplification success rates for weak amplicons that cannot be reliably visualized with
177 commercial dyes (Table 1). The PCR products for each set were pooled and sequenced using
178 MinION (set 1: 7,035,075; set 2: 7,179,121 1D nanopore reads). Both sets were sequenced in
179 two MinION runs. The first run for each set was based on the pooled PCR products for all
180 specimens in the set. It generated 3,069,048 and 4,853,363 reads, respectively. The results of
181 the first run were used to estimate coverage for each PCR product. Products with weak
182 coverage (<=50x) were re-pooled and re-sequenced (set 1: 2,172 amplicons; set 2: 2,211
183 amplicons). This added 3,966,027 and 2,325,758 reads to each set and improved the coverage
184 of many low-coverage barcodes (Fig. 2).

185 The combined data were processed using an improved version of a bioinformatics pipeline
186 introduced in Srivathsan et al. [14]. The improvements led to a higher demultiplexing rate (14%
187 increase for set 1: 898,979 vs. 787,239 reads; 9% increase for set 2: 647,152 vs. 593,131

188 reads) and faster demultiplexing (10X using 4 cores: demultiplexing in 9 min vs 87 min for one
189 of the datasets).

190

191 **2. Assessment of demultiplexing accuracy**

192 We indirectly assessed the accuracy of the demultiplexing pipeline by testing whether reads
193 would be incorrectly demultiplexed into bins belonging to unused tag combinations. This
194 happened for a very small proportion of reads (0.23%: 2,054 of 900,698 reads in set 1; 0.44%:
195 2,837 of 649,587 reads in set 2). Note that such low error rates are unlikely to yield poor quality
196 barcodes given that the average coverage per amplicon was 210X (set 1) and 143X (set 2).
197 Surprisingly, 37% and 69% of these incorrectly demultiplexed reads were due to one tag:
198 GTCCAACTTCAGT although the edit distances between all tag-pairs were high (>=5 bp); i.e., it
199 is currently unclear whether the underperforming tag was due to a primer synthesis issue,
200 systematic sequencing bias, or a wet lab problem (Additional File 1: Fig 1). Out of caution, we
201 provided four additional tag sequences that can be used as replacements (Additional File 2).

202

203 **3. Barcode calling**

204 Demultiplexing all data and calling preliminary barcodes generated 3,797 and 3,476 preliminary
205 "MAFFT barcodes" with >=5X coverage and <1% ambiguous bases. These barcodes were
206 subjected to correction using RACON [31] which yielded the same number of "RACON
207 barcodes". We overall obtained 7,221 MAFFT and RACON barcodes. These preliminary
208 barcodes still contained indel and substitution errors that were corrected with an amino-acid
209 correction pipeline that was first implemented in Srivathsan et al. [14]. It yielded 7,178 AA-
210 corrected MAFFT barcodes ("MAFFT+AA") and 7,194 AA-corrected RACON barcodes
211 ("RACON+AA"). This pipeline rejects barcodes that have five or more consecutive indel errors
212 so that there are fewer corrected than uncorrected barcodes. Finally, the two sets of corrected

213 barcodes were consolidated. This yielded a set of 7,155 consolidated, final barcodes. During
214 this process, the consolidated barcodes where the alignment of MAFFT+AA and RACON+AA
215 barcodes required the insertion of indels were rejected because AA-corrected barcodes are
216 expected to be indel-free. The overall barcoding success rate was thus 82.3% (7,155 barcodes
217 for 8,699 specimens). This was close to the expected 80.7% success rate based on gel
218 electrophoresis; i.e., MinION sequencing consistently produced sequence data for successfully
219 amplified products.

220 A subsequent contamination check via BLAST revealed that of the 7,155 barcodes, 96
221 barcodes were unlikely to be phorid flies (<1.5%). These included 53 barcodes with matches to
222 *Wolbachia, Rickettsia,* nematodes, human, and occasionally insects from other families (e.g.
223 *Drosophila, Hemipyrellia*) and another 43 that did not belong to Phoridae and were incorrectly
224 pre-sorted by parataxonomists. After removal of these, we retained 7,059 confirmed phorid
225 barcodes. Lastly, we inspected the reads obtained for the 92 negative PCR controls (1 per
226 microplate). Five negatives yielded MAFFT barcodes. Four of these had a >97% match to non-
227 phorids (two humans, one fish, one mollusc) and were eliminated. One low coverage (13X)
228 negative survived all filters and matched phorid COI. It was removed after ascertaining that it did
229 not impact the accuracy of the barcodes in the plate. This could be tested by comparing the
230 MinION barcodes for the plate with Illumina barcodes obtained from different PCR products for
231 the same DNA extraction plate (see below).

232 **4. Comparison of MinION barcodes with Illumina barcodes**

233 Illumina barcodes were obtained for 6,251 of the 7,059 specimens with MinION barcodes using
234 a different set of primers that amplified a 313 bp subset of the full-length barcodes; i.e.
235 comparison with MinION sequencing is based on 48% of the MinION sequence. The
236 comparisons showed that the uncorrected MAFFT and RACON barcodes had an accuracy of
237 99.61% and 99.51% (Table 2). Correction of these barcodes with the amino-acid correction

238 pipeline improved the accuracy considerably (>99.9% in all cases). The barcodes were
239 corrected after optimizing a parameter that is here called “namino” because it specifies the
240 length of the AA motifs that is used for correction. Overall, namino=2 was found to optimize
241 overall accuracy while minimizing the number of inaccurate barcodes. We found that
242 MAFFT+AA barcodes were more accurate than RACON+AA barcodes, but MAFFT+AA
243 barcodes contained a much higher number of ambiguous nucleotides (Fig. 3). When
244 RACON+AA and MAFFT+AA barcodes were consolidated, the resulting “consolidated
245 barcodes” were found to be highly accurate (99.99%) and containing few ambiguous bases
246 (median = 0.3%, average=0.46%). These accuracy rates were obtained after excluding the
247 <0.5% specimens that had >3% divergence with corresponding Illumina barcodes. Such
248 barcode discrepancies are likely due to wet-lab errors (e.g., amplification of residual
249 contaminating signals, see details in methods). Note that such errors are regularly observed in
250 large-scale barcoding projects. For examples, a recent study by Hebert et al. [10] using PacBio
251 Sequel for DNA barcoding found that 1.5-1.6% of the specimens had high abundances of non-
252 target sequences.

253 **5. Comparison of MinION and Illumina barcodes at mOTU-level**

254 Given that the barcodes were obtained for the purpose of species richness estimates, we
255 compared the mOTU richness estimated based on the different barcode sets against those
256 obtained with Illumina barcodes. For this purpose, we trimmed the MinION barcode sets to the
257 313 bp fragment that was sequenced using Illumina. mOTU richness was very similar (Table 2).
258 However, comparison of mOTU numbers alone does not imply that the same specimens were
259 grouped into mOTUs obtained with the MinION and Illumina barcodes. One also has to assess
260 whether the contents of the mOTUs are identical. We thus calculated the match ratio for the
261 datasets (3% clustering threshold). We found that all five barcode sets (MAFFT, RACON,
262 MAFFT+AA, RACON+AA, and consolidated barcodes, namino=2) had high match ratios

263 (>0.95). The consolidated and RACON barcodes performed best with match ratios of >0.98
264 (consolidated barcodes: 0.991, RACON: 0.981). However, upon closer inspection the multiple
265 sequence alignment (MSA) for the RACON barcodes contained indels while the consolidated
266 barcodes are insertion-free and contain next to no deletions. Here, single bp deletions were
267 found in the first twenty bps of the barcode for 3/7059 specimens. The largest number of indels
268 was found in the MSA of uncorrected RACON barcodes which indicated that the RACON
269 barcodes retained a fair number of indel errors; i.e., RACON barcodes may not be of sufficient
270 quality for submission to sequence databases. We thus recommend the usage of consolidated
271 barcodes. This recommendation is based on maximizing per-base accuracy (see below),
272 yielding high-quality alignments, and revealing very similar mOTU diversity and composition
273 (high match ratio) when compared to Illumina barcodes.

274 Given the different length of MinION and Illumina barcodes, we also compared the mOTUs
275 obtained by full-length MinION barcodes (658 bp) with the mOTUs obtained with Illumina
276 barcodes for those specimens for which both types of data were available. The match ratio was
277 again high (0.951). For incongruent clusters, we analysed at which distance threshold they
278 would become congruent. We found that all clusters were congruent within the 1.9-3.7% range;
279 i.e., the remaining 345 bp are not showing a major deviation from the signal obtained from the
280 313 bp fragment (Additional File 3). We next characterized if there was an increase in error in
281 the 345 bp stretch of the MinION sequence that could not be directly compared to Illumina
282 sequence: if this were the case, we would expect that spurious base calls would increase
283 genetic distances for specimens. However, we found the opposite: in 18 of 21 cases, the
284 threshold was lowered, i.e., the 345 additional nucleotides reduced the minimum distance in the
285 cluster (Additional File 3).

286 **6. Species richness estimation**

287 After these quality checks, we proceeded to characterize the diversity of phorid flies based on
288 the MinION barcodes of highest accuracy based on comparison with Illumina; i.e., the
289 consolidated barcodes (namino=2). We obtained a mean of 660 mOTUs when the thresholds
290 were varied from 2-4% (2%: 705, 3%: 663, 4%: 613). These thresholds are widely used in the
291 literature, but also supported by empirical data from GenBank. GenBank has 12,072 phorid
292 sequences with species-level identifications belonging to 106 species. The intraspecific
293 variability is overwhelmingly <3% (>95% of pairwise distances) and the match ratios between
294 mOTUs and species identifications from GenBank are maximized for clustering thresholds of 2 -
295 3% (Additional File 1: Fig S2, S3). In addition to clustering the barcodes based on *a priori*
296 thresholds, we also used species delimitation based on Poisson Tree Processes (PTP) to
297 estimate the number of species for the phorids from the trap. It yielded even higher richness
298 estimate of 747 putative species than the threshold-based methods. Lastly, we used species
299 accumulation and Chao 1 curves (mOTUs at 3%) to estimate the full phorid diversity of the
300 Ugandan site. We find that the curves have yet to reach a plateau, but the shape of the curves
301 suggests an estimated diversity of ~1,000 species of Phoridae at a single field site in Uganda,
302 collected by one Malaise trap (Fig. 4).

303 **7. Paralogy check**

304 We found that the Illumina were translatable which is not expected for sequences obtained for
305 old NuMTs. In addition, the congruence between the mOTUs estimated based on sequences for
306 two different amplicons of different lengths and different primer specificity is very high. This
307 would not be expected if NuMTs were regularly amplifying. We also scrutinized the read sets for
308 Illumina amplicons for the presence of secondary phorid signal. We found such signal in 7%
309 (30) of the 406 mOTUs with multiple specimens. Such signal can be caused by paralogs or low-
310 level lab contamination when small amounts of template from one well contaminates the PCR
311 reaction in another well. We suspect that much of the secondary signal is caused by the latter,

312 but it is arguably more important that the level of secondary signal is sufficiently low that it could
313 not significantly lower the overall species richness estimate of the site even if all secondary
314 signal was caused by paralogy (Additional File 4).

315 **8. Congruence with morphology**

316 We conducted a morphological check of 100 randomly selected clusters (>1,500 specimens).
317 We found that 6 of the 100 clusters contained, among other specimens, a single misplaced
318 specimen. There was one cluster of four specimens that appeared to consist of a mixture of
319 three morpho-species. This implies that 9 of the >1,500 examined barcoded specimens were
320 misplaced due to lab contamination. This morphological check took ca. 30 hours. mOTUs based
321 on barcodes are expected to lump those species that recently speciated and split species with
322 well-differentiated populations [32]. This means that taxonomists working with mOTUs should
323 check for signs of lumping and splitting in closely related taxa. This requires morphological
324 examination of a subset of specimens whose selection is guided by genetic information. This is
325 aided by keeping closely related mOTUs physically together. In the case of phorids this can be
326 done by slide mounting representative specimens from the sub-clusters. This is here illustrated
327 by describing one species based on a complex cluster.
328

329 **New Species Description**

330 During the morphological work, a distinctive new species of *Megaselia* was found. A mOTU-
331 specific haplotype network was constructed and informed on which specimens should be
332 studied based on morphology. The new species is here described. To continue reducing
333 redundancy and ambiguity in species descriptions, the description of this species has excluded
334 the character table from the method previously established for *Megaselia* [33-35] and uses a
335 molecular and photographic description. Photographs are a key element in descriptions for
336 large, diverse groups [36], where verbose descriptions require much time while remaining

insufficiently diagnostic. Most characters that would have been in table form are clearly visible in the photographs provided.

Megaselia sepsioides Hartop sp. n.

urn:lsid:zoobank.org:pub:ED268DF2-A886-4C31-A4FB-6271C382DECE

DNA barcode for UGC0005996 (GenBank accession: MN403533)

actttatattttatttttggagcttgagctggaatagtaggtacttccttaagaatcataattcgtgctgaattaggacacccaggagcacttat
tggtgatgaccaaatttataatgtgattgttactgcacatgcttttattataattttttttatagtaatacctattataataggaggttttggtaattg
acttgtacctttaatattaggagccccagatatggcattccctcgaatgaataatataagtttttgaatattacctccttctttaactcttttatta
gccagaagtatagtagaaaatggagctggaactggttgaacagtttatcctcctttatcttctagaatcgctcatagtggagcttctgttgat
ttagcaattttctctcttcatttagctggaatttcatctattttaggagctgtaaattttattacaacaattattaatatacgatcatcaggtattaca
tttgaccgaatacctctatttgtttgatctgtaggtattacagctttattgctactcttatcacttcctgttttagctggtgctattacaatactattaa
cagaccgaaattttaatacttcattttttgacccagcaggaggaggagatccaattttataccaacatttattc

Fig. 5, 6, 7

Diagnosis

Well characterized by the following combination of characters: with unique semi-circular expansion with modified peg-like setae on the forefemur (Fig. 5, b), hind tibia strongly constricted (Fig. 5, d and e), and abdomen narrow and elongate. Three haplotypes were examined; variations in setation were observed between the main cluster and two haplotypes (Fig. 6, 7). Only single specimens of the two distinct haplotypes are available; more specimens will be necessary to determine if these are eventually removed as distinct species or fall within a continuum of intraspecific variation.

Material Examined

Holotype. ♂, UGANDA: Kamwenge, Kibale National Park (00°33'54.2"N 30°21'31.3"E,1530 m), iii-xii.2010, Olavi Kurina & Swaibu Katusabe (LKCNHM UGC0005996).

Paratypes. 7 ♂, UGANDA: Kamwenge, Kibale National Park (00°33'54.2"N 30°21'31.3"E,1530 m), iii-xii.2010, Olavi Kurina & Swaibu Katusabe (LKCNHM: UGC0012899, UGC0012244, UGC0012568, UGC0003003, UGC0005864, UGC0012937, UGC0012971).

Distribution

Known from a single site in Kibale National Park, Uganda.

Biology

Unknown.

Etymology

Name suggested by Yuchen Ang for the sepsid-like (Diptera: Sepsidae) foreleg modification.

DISCUSSION

Remarkably high diversity of Phoridae in Kibale National Park

The full extent of the world's biodiversity is poorly understood because many hyperdiverse taxa are data-deficient. One such hyperdiverse clade is phorid flies. We here reveal that even a modest amount of sampling (one Malaise trap placed in Kibale National Park, Uganda) can lead to the discovery of >650 putative species. This diversity constitutes 150% of the described phorid diversity of the entire Afrotropical region (466: [28]). Note that the ca. 7,000 barcoded specimens covered in our study only represent 8 one-week samples obtained between March 2010 and February 2011. There are an additional 44 weekly samples that remain un-

388 sequenced. We thus expect the diversity from this single site to eventually exceed 1,000
389 species. This prediction is supported by a formal species-richness estimation based on the
390 available data (Fig. 4). Such extreme diversity from a single site raises the question of whether
391 these numbers are biologically plausible and/or whether they could be caused by unreliable
392 data or species delimitation methods.
393
394 We would argue that they are both biological plausible and analytically sound. If a single garden
395 in a temperate city like Cambridge (UK) can have 75 species and the urban backyards of Los
396 Angeles 82, observing 10-15 times of this diversity at a site in a tropical National Park does not
397 appear unrealistic. Our proposition that there are >1,000 species at a single site in Kibale
398 National Park is further supported by the results of the Zurqui survey in Costa Rica which
399 revealed 404 species of Phoridae without completing the species discovery process [26].
400 Furthermore, we are confident that our species richness estimate is not an artefact of poor data
401 quality because the high species richness estimate is supported by both Illumina and MinION
402 barcodes generated independently using different primer pairs. It is furthermore stable to
403 modifications of sequence clustering thresholds which are widely used across Metazoa and
404 here shown to be appropriate for phorid flies based on the available Genbank data [37]. Lastly,
405 we checked 100 randomly chosen mOTUs for congruence between molecular and
406 morphological evidence. We find that 93% of the clusters and >99% of specimens are
407 congruently placed (six of the seven cases of incongruence involved single specimens). This is
408 in line with congruence levels that we observed previously for ants and odonates [4, 7].
409
410 The high species richness found in one study site inspired us to speculate about the species
411 diversity of phorids in the Afrotropical region. This is what Terry Erwin did when he famously
412 estimated a tropical arthropod fauna of 30 million species based on his explorations of beetle
413 diversity in Panama [38]. Such extrapolations are arguably useful because they raise new

414 questions and inspire follow-up research. Speculation is inevitable given that it remains
415 remarkably difficult to estimate the species richness of diverse taxa [39]. This is particularly so
416 for the undersampled Afrotropical region which comprises roughly 2,000 squares of 100 km^2
417 size. In our study, we only sampled a tiny area within one of these squares and observed >650
418 species which likely represent a species community that exceeds >1,000 species. Note that
419 Malaise traps only sample some phorid species because many specialist species (e.g., termite
420 inquilines) rarely enter such traps. In addition, the estimated 1,000 species that can be caught in
421 a single Malaise trap are also only a subset of the species occurring in the remaining habitats of
422 the same 100 km^2 grid cell. Overall, it seems thus likely that the 100 km^2 will be home to several
423 thousand species of phorids. If we assume that on average each of the two-thousand 100 km^2
424 grid cells of the Afrotropical Region has "only" 100 endemic phorid species, the endemic phorids
425 alone would contribute 200,000 species of phorids to the Afrotropical fauna without even
426 considering the contributions by the remaining species with a wider distribution. What is even
427 more remarkable is that most of the diversity would belong to a single genus. We find that 90%
428 of the newly discovered species and specimens in our sample belong to the genus *Megaselia*
429 as currently circumscribed. Unless broken up, this genus could eventually have >100,000
430 Afrotropical species. All these estimates would only be lower if the vast majority of phorid
431 species had very wide distributions and/or the average number of species in 100 km^2 grid cells
432 would be more than one order of magnitude lower than observed here. However, we consider
433 this unlikely given that many areas of the Afrotropical region are biodiverse and cover a wide
434 variety of climates and habitats which increases beta diversity.
435
436 Unfortunately, most of this diversity would have remained overlooked using the traditional
437 taxonomic workflow because it is not well suited for taxa with high species diversity and
438 specimen abundances. This means that the phorid specimens from the Kibale National Park
439 Malaise trap would have remained in the unsorted residues for decades or centuries. Indeed,

440 there are thousands of vials labelled “Phoridae” shelved in all major museums worldwide.
441 Arguably, it is these unprocessed samples that make it so important to develop new rapid
442 species-level sorting methods. We here favour sorting with “NGS barcodes” [4] because it would
443 allow biologists to work through the Malaise trap residues in Natural History museums. These
444 residues will almost certainly contain several times the number of species that have already
445 been described. We predict that there will be two stages to species discovery with NGS
446 barcodes. The first is species-level sorting which can yield fairly accurate estimates of species
447 diversity and abundance [4, 8]. Many biodiversity-related questions can already be addressed
448 based on these data. The second phase is the refinement of mOTUs based on morphological
449 testing with subsequent species identification (described species) or species description (new
450 species). Given the large number of new species, this will require optimized “turbo-taxonomic”
451 methods. Fortunately, new approaches to large-scale species description are being developed
452 and there are now a number of publications that describe ~100 or more new species [36, 40-
453 42].
454
455 *MinION sequencing and the “reverse workflow”*
456 MinION barcodes can be obtained without having to invest heavily into sequencing facilities and
457 laboratories fully equipped for barcoding specimens with MinION can be mobile and operate
458 under difficult conditions in the field or field stations [15-18]. The technology is thus likely to
459 become important for the “democratization” of biodiversity research because the data are
460 generated quickly enough that they can be integrated into high school and citizen scientist
461 initiatives. Based on our data, we would also argue that MinION is now suitable for wide-spread
462 implementation of the “reverse-workflow” where all specimens are sequenced before mOTUs
463 are assessed for consistency with morphology. Reverse-workflow differs from the traditional
464 workflow in that it relies on DNA sequences for sorting all specimens into putative species while
465 the traditional workflow starts with species-level sorting based on morphology; only some

466 morpho-species are subsequently examined with a limited amount of barcoding. We would
467 argue that the reverse-workflow is more suitable for handling species- and specimen-rich clades
468 because it requires less time than high-quality sorting based on morphology which often
469 involves genitalia preparations and slide-mounts. For example, even if we assume that an
470 expert can sort and identify 50 specimens of unknown phorids per day, the reverse workflow
471 pipeline would increase the species-level sorting rate by >10 times (based on the extraction and
472 PCR of six microplates per day). In addition, the molecular sorting can be carried out by lab
473 personnel trained in amplicon sequencing while accurate morpho-species sorting requires
474 highly trained taxonomic experts. Yet, even highly trained experts are usually not able to match
475 morphologically disparate males and females belonging to the same species (often one sex is
476 ignored in morphological sorting) while the matching of sexes (and immatures) is an automatic
477 and desirable by-product of applying the reverse workflow [7]. All these benefits can be reaped
478 rapidly. One lab member can amplify the barcode of 600-1,000 specimens per day (2-2.5 weeks
479 for 8,000 specimens). Obtaining DNA sequences requires ca. one week because it involves two
480 cycles of pooling and sequencing on two MinION flowcells followed by two cycles of re-pooling
481 and sequencing of weak amplicons. The bioinformatics work requires less than one week.
482
483 One key element of the reverse workflow is that the vials with specimens that have haplotype
484 distances <5% are physically kept together. This helps when assessing congruence between
485 mOTUs and morphology. Indeed, graphical representations of haplotype relationships (e.g.,
486 haplotype networks) can guide the morphological re-examination as illustrated in our description
487 *of Megaselia sepsioides* (Fig. 7). Here, eight specimens belonging to seven haplotypes were
488 dissected and the most dissimilar haplotypes were studied in order to test whether the data
489 support the presence of one or two species. Variations in setation were observed (Fig. 6) but
490 they were consistent with intraspecific variation. Note that the morphological examination of

491 clusters was straightforward because the use of QuickExtract™ for DNA extractions ensures
492 morphologically intact specimens.
493
494 *Large-scale species discovery using MinION 1D reads*
495 Our results suggest that MinION's 1D sequencing yields data of sufficient quality for producing
496 DNA barcodes that can be used for large-scale species discovery. Through the development of
497 new primer-tags, re-pooling of low coverage amplicons, and an improved bioinformatics
498 workflow, we here increased the barcoding capacity of a MinION flowcell by 700% from 500
499 specimens (Srivathsan et al., [14]: $1D^2$ sequencing) to ~3,500 specimens. This is achieved
500 without a drop in accuracy because the error correction pipeline is effective at eliminating most
501 of the errors in the 1D reads (ca. 10%). Indeed, even the initial estimates of barcodes ("MAFFT"
502 & "RACON") have very high accuracy (>99.5%) when compared to Illumina data, while the
503 accuracy of consolidated barcodes is even higher (>99.9%). Note that the accuracy of the
504 barcodes obtained in this study are even higher than what was obtained with $1D^2$ sequencing in
505 Srivathsan et al. (99.2%) [14]. We suspect that this partially due to improvements in MinION
506 sequencing chemistry and base-calling, but our upgraded bioinformatics pipeline also helps
507 because it increases coverage for the amplicons. This is welcome news because 1D library
508 preparations are much simpler than the library preps for $1D^2$. In addition, $1D^2$ reads are currently
509 less suitable for amplicon sequencing [43]. Overall, the accuracy of our MinION barcodes are
510 also comparable with what can be obtained with PacBio Sequel ([10]: Additional File 1: Figure
511 S5). This platform also allows for obtaining full-length barcodes, but the cost of purchasing and
512 maintaining a PacBio sequencer is very high.
513
514 Using the workflow described here, MinION barcodes can be generated rapidly and at a low
515 sequencing cost of <0.35 USD per barcode. Molecular cost of PCR is 0.16 USD per reaction [4]
516 while QuickExtract™ reagent costs 0.06 per specimen. These properties make MinION a

517 valuable tool for species discovery whenever a few thousand specimens (<5,000) must be
518 sorted to species. Even larger-scale barcoding projects are probably still best tackled with
519 Illumina short-read or PacBio's Sequel sequencing [4, 10, 11] because the barcoding cost is
520 even lower. However, both require access to expensive sequencing instruments, sequencing is
521 thus usually outsourced, and the users usually have to wait for several weeks in order to obtain
522 the data. This is not the case for barcoding with MinION, where most of the data are collected
523 within 10 hours of starting a sequencing run. Another advantage of the MinION pipeline is that it
524 only requires basic molecular lab equipment including thermocyclers, a magnetic rack, a Qubit,
525 a custom-built computational device for base-calling ONT data ("MinIT"), and a laptop (total cost
526 of lab <USD 10,000). Arguably, the biggest operational issue is access to a sufficiently large
527 number of thermocyclers given that a study of the scale described here involves amplifying PCR
528 products in 92 microplates (=92 PCR runs).
529
530 Our new workflow for large-scale species discovery is based on sequencing the amplicons in
531 two sequencing runs. The second sequencing run can re-use the flowcell that was used for the
532 first run. Two runs are desirable because they improve overall barcoding success rates. The
533 first run is used to identify those PCR products with "weak" signal (=low coverage). These weak
534 products are then re-sequenced in the second run. This dual-run strategy overcomes the
535 challenges related to sequencing large numbers of PCR products: the quality and quantity of
536 DNA extracts are poorly controlled and PCR efficiency varies considerably. Pooling of products
537 ideally requires normalization, but this is not practical when thousands of specimens are
538 handled. Instead, one can use the real-time sequencing provided by MinION to determine
539 coverage and then boost the coverage of low-coverage products by preparing and re-
540 sequencing a separate library that contains only the low coverage samples. Given that library
541 preparations only require <200 ng of DNA, even a pool of weak amplicons will contain sufficient
542 DNA. This ability to re-pool within days of obtaining the first sequencing results is a key

543 advantage of MinION. The same strategy could be pursued with Illumina and PacBio but it
544 would take a long time to obtain all the results because one would have to wait for the
545 completion of two consecutive runs.

546

547 **METHODS**

548 **1. Sampling**

549 Samples were collected by a single Townes-type Malaise trap [44], in the Kibale National Park,
550 close to Kanyawara Biological Station in the evergreen primeval forest at an altitude of 1513 m
551 (00°33'54.2"N 30°21'31.3"E) (Fig. 4). Kibale National Park is characterized as a fragment of
552 submontane equatorial woodland [45]. Temperatures in Kibale range from 16°C to 23°C (annual
553 mean daily minimum and maximum, respectively) [46]. The Malaise trap was checked every
554 week when the collecting bottle with the material was replaced by a resident parataxonomist
555 ([47]: Mr. Swaibu Katusabe). Subsequently, the material was collected and transferred in
556 accordance with approvals from the Uganda Wildlife Authority (UWA/FOD/33/02) and Uganda
557 National Council for Science and Technology (NS 290/ September 8, 2011), respectively. The
558 material was thereafter sorted to higher-level taxa. Target taxa belonging to Diptera were sorted
559 to family and we here used the phorid fraction. The sampling was done over several months
560 between 2010 and 2011. For the study carried out here, we only barcoded ca. 30% of the phorid
561 specimens. The flies were stored in ethyl alcohol at -20-25°C until extraction.

562 **2. DNA extraction**

563 DNA was extracted using whole flies. The fly first taken out from the vial and washed in Milli-Q®
564 water prior to being placed in a well of a 96 well PCR plate. DNA extraction was done using 10
565 ul of QuickExtract™ (Lucigen) in a 96 well plate format and the whole fly was used to extract
566 DNA. The reagent allows for rapid DNA extraction by incubation (no centrifugation or columns

567 are required). The solution with the fly was incubated at 65°C for 15 min followed by 98°C for 2
568 min. No homogenization was carried to ensure that the intact specimen was available for
569 morphological examination.
570
571 **3. MinION based DNA barcoding**
572 *I. Polymerase Chain Reactions (PCRs)*
573 Each plate with 96 QuickExtract™ extracts (95 specimens and 1 control, with exception of one
574 plate with no negative and one partial plate) was subjected to PCR in order to amplify the 658
575 bp fragment of COI using LCO1490 5' GGTCAACAAATCATAAAGATATTGG 3' and HCO2198
576 5' TAAACTTCAGGGTGACCAAAAAATCA 3' [48]. This primer pair has had high PCR success
577 rates for flies in our previous study [14] and hence was chosen for phorid flies. Each PCR
578 product was amplified using primers that included a 13 bp tag. For this study, 96 thirteen-bp
579 tags were newly generated in order to allow for upscaling of barcoding; these tags allow for
580 multiplexing >9200 products in a single flowcell of MinION through unique tag combinations
581 (96x96 combinations). To obtain these 96 tags, we first generated one thousand tags that
582 differed by at least 6 bp using BarcodeGenerator [49] However, tag distances of >6 bp are not
583 sufficiently distinct because they do not take into account MinION's propensity for creating
584 errors in homopolymer stretches and other indel errors. We thus excluded tags with
585 homopolymeric stretches that were >2 bp long. We next used a custom script to identify tags
586 that differed from each other by indel errors. Such tags were eliminated recursively to ensure
587 that the final sets of tags differed from each other by >=3bp errors of any type (any combination
588 of insertions/deletions/substitutions). This procedure yielded a tag set with the edit-distance
589 distribution shown in Additional File 1: Fig S1 [minimum edit distance (as calculated by *stringdist*
590 module in Python) of 5 nucleotides (38.5%) which is much higher than Nanopore error rates].
591 Lastly, we excluded tags that ended with "GG" because LCO1490 starts with this motif. Note
592 that longer tags would allow for higher demultiplexing rates, but our preliminary results on PCR

593 success rates suggested that the use of long tags reduced amplification success (one plate: 7%
594 drop).
595
596 The PCR conditions for all amplifications were as follows, reaction mix: 10 µl Mastermix
597 (CWBio), 0.16 µl of 25mM $MgCl_2$, 2 µl of 1 mg/ml BSA, 1 µl each of 10 µM primers, and 1ul of
598 DNA. The PCR conditions were 5 min initial denaturation at 94°C followed by 35 cycles of
599 denaturation at 94°C (30 sec), annealing at 45°C (1 min), extension at 72°C (1 min), followed by
600 final extension of 72°C (5 min). For each plate, a subset of 7-12 products were run on a 2%
601 agarose gel to ensure that PCRs were successful. Of the 96 plates studied, 4 plates were
602 excluded from further analyses as they had <50% amplification success and one plate was
603 inadvertently duplicated across the two runs.
604
605 *II. MinION sequencing*
606 We developed an optimized strategy for nanopore sequencing during the study. For the initial
607 experiment (set 1), we sequenced amplicons for 4,275 phorid flies. For this, all plates were
608 grouped by amplicon strength as judged by the intensity of products on agarose gels and
609 pooled accordingly (5 strong pools + 2 weak pools). The pools were cleaned using either 1X
610 Ampure beads (Beckman Coulter) or 1.1X Sera-Mag beads (GE Healthcare Life Sciences) in
611 PEG and quantified prior to library preparation. The flowcell sequenced for 48 hours and yielded
612 barcodes for ~3200 products, but we noticed lack of data for products for which amplification
613 bands could be observed on the agarose gel. We thus re-pooled products with low coverage
614 (<=50X), prepared a new library and sequenced them on a new flowcell. The experiment was
615 successful. However, in order reduce sequencing cost and improve initial success rates, we
616 pursued a different strategy for the second set of specimens (4,519 specimens). In the first
617 sequencing run, we stopped the sequencing after 24 hours. The flowcell was then washed using
618 ONT's flowcell wash kit and prepared for reuse. The results from the first 24 hours of

619 sequencing were then used to identify amplicons with weak coverage. They were re-pooled, a
620 second library was prepared, and sequenced on the pre-used and washed flowcell.
621
622 Pooling of weak products with <=50X coverage was done as follows: We located (1) specimens
623 <=10X coverage (set 1: 1,054, set 2: 1,054) and (2) specimens with coverage between 10X and
624 50X (set 1: 1,118, set 2: 1,065). Lastly, we also created a (3) third pool of specimens with
625 "problematic" products that were defined as those that were found to be of low accuracy during
626 comparisons with Illumina barcodes and those that had high levels of ambiguous bases (>1%
627 ambiguous bases during preliminary barcode calling). Very few amplicons belonged to this
628 category (set 1: 68, set 2: 92). In order to efficiently re-pool hundreds of specimens across
629 plates we wrote a script that generates visual maps of the microplates that illustrate the wells
630 where the weak products are found (available in github repository for *miniBarcoder*).
631
632 Library preparation and sequencing: We used the SQK-LSK109 ligation sequencing kit (Oxford
633 Nanopore Technologies) for library preparation and sequencing. Our first experiment on set 1
634 used 1 ug of starting DNA while all other libraries used 200 ng pooled product. Library
635 preparation was carried out as per manufacturer's instructions with one exception: the various
636 clean-up procedures at the end-prep and ligation stages used 1X Ampure beads (Beckmann
637 Coulter) instead of 0.4 X as suggested in the instructions because the amplicons in our
638 experiments were short (~735 bp with primers and tags). The sequencing was carried out using
639 MinION sequencer with varying MinKNOW versions between August 2018 - January 2019.
640 Fast5 files generated were uploaded onto a computer server and base-calling was carried out
641 using Guppy 2.3.5+53a111f. No quality filtering criteria were used. Our initial work with Albacore
642 suggested that quality filtering improved demultiplexing rate but overall more reads could be
643 demultiplexed without the filtering criterion.
644

645 *III. Data analyses for MinION barcoding*

646 We attempted to demultiplex the data for set 1 using *minibar* [50], however it was found to
647 demultiplex only 1,039 barcodes for the 4275 specimens (command used: python
648 ../minibar/minibar.py -F -C -e 2 minibar_demfile_1 phorid_run1ab.fa_overlen599 > out). This
649 success rate was so low that we discontinued the use of *minibar*. Instead, we analysed the data
650 using an improved version of *miniBarcoder* [14]. This pipeline starts with a primer search with
651 *glsearch36,* followed by identifying the "sequence tags" in the flanking nucleotide sequences,
652 before the reads are demultiplexed based on tags. For the latter, errors of up to 2 bp are
653 allowed. These "erroneous" tags are generated by "mutating" the original tags 96 tags to
654 account for all possible insertions/deletions/substitutions. The sequence tags are matched with
655 this set of input tags + tag mutants. This speeds up demultiplexing as it does not have to align
656 each tag. When comparing the performance of *miniBarcoder* with *minibar*, we found that using 4
657 cores, *miniBarcoder* could demultiplex data in <10 minutes while *minibar* required 74 minutes in
658 one. Both pipelines demultiplexed similar numbers of reads: 898,979 reads using *miniBarcoder*,
659 while 940,568 HH reads of *minibar* (56,648 reads in multiple samples). The demultiplexed reads
660 were aligned using MAFFT v7 (--op 0) (here v7) [51]. In order to improve speed, we only used a
661 random subset of 100 reads from each demultiplexed file for alignment. Based on these
662 alignments, a majority rule consensus was called to obtain what we call "MAFFT barcodes".

663

664 Other studies usually incorporate a step of clustering of data at low thresholds (e.g. 70% by
665 Maestri et al. 2019 [18]) in order to account for the read errors produced by MinION. The
666 subsequent analysis is then carried out on the cluster that has the largest number of reads. We
667 deviate from this approach because it requires high coverage. In our barcoding pipeline, we
668 assess congruence for each base-pair by firstly eliminating the MAFFT gap-opening penalty (--
669 op 0); this allows for all data to be used when calling the consensus [14]: this gap opening
670 penalty essentially treats indel and substitutions similarly and staggers the alignment. Any base

671 that is found in <50% of the position is called as an ambiguity; i.e., the majority-rule criterion is
672 applied for each site instead of filtering at the read level which is based on averages across all
673 bases. This site-specific approach maximizes data use by allowing barcodes to be called at
674 much lower coverage levels than with other pipelines (5-20X coverage compared to >200x
675 coverage in Maestri et al. 2019 [18]), while also identifying contaminated specimen barcodes.
676
677 In our pipeline, MAFFT barcodes are improved by mapping all the reads back to the barcode
678 using GraphMap (here v0.5.2) [52] and calling the consensus using RACON (here, v1.3.1) [31].
679 This yields what we call "RACON barcodes". Both MAFFT and RACON barcodes are subject to
680 further correction based on publicly available barcodes in GenBank. These corrections are
681 advisable in order to fix the remaining indel errors. The correction takes advantage of the fact
682 that COI sequences are translatable; i.e., an amino acid-based error correction pipeline can be
683 used (details can be found in Srivathsan et al. [14]). Applying this pipeline to MAFFT and
684 RACON barcodes, respectively, yields MAFFT+AA and RACON+AA barcodes. Lastly, these
685 barcodes can be consolidated into "consolidated barcodes".
686 The version of the pipeline in Srivathsan et al. [14] was modified as follows:
687 a. *Tackling 1D reads for massively multiplexed data:* We developed ways for correcting for the
688 increased number of errors in 1D reads by identifying objective ways for quality assessments
689 based on the MinION data and publicly available data (GenBank): (1) The GraphMap max error
690 was increased from 0.05 to 0.15 to account for error rates of 1D reads. (2) We modified the
691 approach for calculating consolidated barcodes. These consolidated barcodes are generated by
692 aligning translatable MAFFT and RACON barcodes. We then use the strict consensus of
693 MAFFT+AA and RACON+AA barcodes in order to resolve conflicts between MAFFT and
694 RACON barcodes if there are substitution conflicts. In Srivathsan et al. [14] we accepted
695 MAFFT+AA barcodes in cases of conflict, but for the 1D data we found that MAFFT+AA
696 barcodes had more ambiguities than RACON+AA barcodes which could be resolved via

calculating a strict consensus. We increased the gap-open penalty from default 1.53 to 3, as the MAFFT+AA and RACON+AA barcodes are translatable and their alignments should not contain indels. Lastly if the alignment still contains indels despite the increase in gap opening penalty the barcode is rejected. (3) We assessed how different window sizes can impact the amino-acid correction pipeline by varying the “namino” parameter (number of AA to be inspected in each side of an indel). (4) During the amino-acid correction, we introduced a final sequence translation check to ensure that a translatable product was obtained: if stop codons were still present these would be replaced by ambiguities. These affected four barcodes in our study.

b. Demultiplexing rate: (1) We introduced a “homopolymer compression” of the putative tag sequences in order to improve demultiplexing rates. After primer searches, the old pipeline used to identify the flanking 13 bps that were likely to be tag sequence. Instead we now use a 20 bp flanking sequence and then compress any homopolymer >3bp before searching for 13 bp tags. (2) We now analyze very long reads that can be formed when two amplicons ligate during library preparation. Long reads are split into size classes of <1,300, >1,300 and <2,000. These settings were set based on 658 bp barcode of COI: the total product size including tags and primers is 735 bp, and hence, a sequence with two products ligated to each other is expected to be 1,470 bp long. The sequences were split in a manner that ensured that the tags of first product are not affecting the tag found in the second, i.e., primer search for second product was conducted after the first 650 bp of the sequence. Currently, this option is only available for reads that consist of two ligated products.

c. Processing speed and memory requirements: (1) For primer identification we now limit the searches to the first and last 100 bp of each read which allowed for improving speed of the primer search. (2) We parallelized the process of demultiplexing and MAFFT barcode calling using multiprocessing in python. This allows for fast demultiplexing whenever computational

723 power is limited. (3) We optimized the pipeline with regard to memory consumption and ensured
724 that all processes are applied to batches of <=20,000 sequences. The latter modification is
725 needed given the rapid increase in MinION output and batch processing is scalable with
726 increased output.
727

728 **4. Assessment of demultiplexing accuracy**

729 Demultiplexing accuracy was assessed by trying to demultiplex reads into bins representing
730 unused tag combinations: 96x96 tags combinations were designed but set 1 used only 45 tags
731 with LCO1490. This allowed for an assessment if *miniBarcoder* would erroneously assign reads
732 for the unused remaining 51X96 combinations. Set 2 used 48 tags thus allowing us to assess if
733 the demultiplexing pipeline erroneously found the remaining 48X96. Lastly one plate used only
734 55 tags associated with HCO2198. Overall, we could assess demultiplexing accuracy
735 associated with 80/96 tags.

736 **5. Illumina Based NGS Barcoding for validation**

737 In order to validate MinION barcodes and optimize error correction strategies, we used
738 reference COI barcodes obtained via Illumina sequencing for the same QuickExtract™ DNA
739 extractions. Illumina sequencing was carried out for a 313 bp fragment of the same COI
740 barcoding region using m1COIintF: 5'-GGWACWGGWTGAACWGTWTAYCCYCC-3' [53] and
741 modified jgHCO2198: 50-TANACYTCNGGRTGNCCRAARAAYCA-3 [54]. We recently
742 conducted an extensive analysis to understand if a 313 bp minibarcode is able to provide similar
743 identifications and species delimitations as 658 bp barcodes and found that minibarcodes
744 performing equally well as full-length barcodes when examining >5,000 species [55].

745 Tagged primers were used for the PCRs as specified in Wang et al. (2018) [4]. The PCR mix
746 was as follows: 4 µl Mastermix from CWBio, 1µl of 1 mg/ml BSA, 1µl of 10 µM of each primer,
747 and 1ul of DNA. PCR conditions: 5 min initial denaturation at 94°C followed by 35 cycles of

748 denaturation at 94°C (1 min), 47°C (2 min), 72°C (1 min), followed by final extension of 72°C (5
749 min). The PCR products were pooled and sequenced along with thousands of other specimens
750 in a lane of HiSeq 2500 (250 bp PE sequencing). The data processing followed Wang et al.
751 (2018) [4]: paired end reads were merged using PEAR (v 0.9.6) [56], reads were demultiplexed
752 by an in-house pipeline that looks for perfect tags while allowing for 2 bp mismatches in primer
753 sequence. For each sample, demultiplexed reads are merged to identify the most dominant
754 sequence with >50X dataset coverage and 10X coverage for the sequence, and a barcode is
755 accepted only if this sequence is 5X as common as the next most common sequence.
756 Demultiplexed reads with >10x coverage were also per sample were retained for analyses of
757 contaminations and paralogs.

758 **6. Assessment of MinION barcodes and mOTU delimitations**

759 Both MinION and Illumina barcodes were subject to contamination check. For MinION barcodes
760 we used preliminary MAFFT barcodes given that this is the largest barcode set. Barcodes were
761 matched to GenBank using BLASTN and taxonomic classifications were assigned using
762 readsidentifier [57]. Any barcode with >95% match to a non-phorid sequence was excluded
763 from the dataset. Furthermore, if any barcode best matched to bacteria, it was also excluded.
764 Lastly, in cases where the best BLAST matches were below 95% and no phorid sequence was
765 in the top 100 BLAST hits, we retrieved the specimen and examined in morphologically to
766 determine if a non-phorid had been sequenced (=pre-sorting error).
767
768 MinION barcodes were assessed by scripts provided in the *miniBarcoder* package
769 (assess_corrected_barcodes.py and assess_uncorrected_barcodes.py). For uncorrected
770 barcodes, this was done by aligning barcodes to reference Illumina barcodes using dnadiff [58].
771 For corrected barcodes (+AA), we used MAFFT to obtain pairwise alignments. This allowed us
772 to compare per base accuracy. Here we excluded those barcodes that had >3% difference

773 between MinION and Illumina barcodes. These are likely to be caused by wetlab error
774 whenever a different product as the Illumina and MinION barcodes were amplified using
775 different primers (<0.5% of specimens) as discussed here: for consolidated barcodes 25/6,251
776 specimens are involved in such >3% distances in the comparisons of consolidated barcodes
777 with Illumina barcodes. If these distances were a result of consensus errors, sequences are
778 unlikely to create consensus that are identical to other specimens. 21/25 specimens have
779 identical sequences to some other specimen and two are within 0.6% of another. By matching
780 MinION barcodes to Illumina's read set for each sample (>=10 counts), we also find that many
781 of the signals being picked up by HCO-LCO are in the Illumina data at low frequencies (in 15/25
782 cases, including one of the two cases that remain unaccounted) that was generated using
783 different primers (Additional File 5). We do not include these for consensus quality, but instead
784 consider them as misplaced sequences.

785 We were furthermore interested in understanding how mOTU delimitation is affected by error
786 correction. Barcodes were aligned using MAFFT and MinION barcodes were further trimmed to
787 the 313 bp region of the Illumina barcode. mOTU delimitation was done at 2, 3 and 4% using
788 SpeciesIdentifier (objective clustering) [59]. mOTU richness was estimated and we furthermore
789 calculated match ratio between two sets of clusters [60]. Match ratio is given by $\frac{2N_{match}}{N_1+N_2}$. For
790 consolidated barcodes, we also calculated the match ratio between mOTU estimates by full
791 length barcodes and Illumina barcodes (313 bp). If the mOTUs were inconsistent we also
792 identified the distance threshold for which they became consistent.

793 **7. Paralog check**

794 Copies of mitochondrial sequences in nuclear genomes (NuMTs, paralogs) can lead to inflated
795 species richness estimation if the mitochondrial gene amplifies in one specimens and the NuMT
796 copy in another specimen that is conspecific. If the sequence copies are sufficiently dissimilar,

797 the two specimens will be placed in two mOTUs although they were conspecific. In our study,
798 multiple checks are used to avoid inflated diversity estimates based on NuMTs. Firstly, we
799 amplify COI sequences of different lengths using two different primer pairs and then check
800 whether the resulting mOTUs are congruent. Congruence would not be expected if the primers
801 have similar affinity to the mitochondrial and nuclear copy of the gene. Secondly, the Illumina
802 read sets were obtained for an amplicon generated with highly degenerate primers. This
803 increases the chance for co-amplification of paralogs. For each demultiplexed set, we obtained
804 the unique sequences that had >=10X coverage. All secondary were matched against the
805 barcode sequences using BLASTN, e-value 1e-5, perc_identity 99%, hit length >=300. If
806 secondary signals for a specimen belonged to a different specimen these could be low level
807 contaminations or paralogs. However, if secondary sequences from multiple specimens of one
808 cluster match to a different cluster, the likelihood that they are paralogs is higher. Note,
809 however, that this technique does not allow for distinguishing between low-level contamination
810 and paralogs.

811 **8. Species richness estimation**

812 The most accurate set of barcodes were used for assessing the overall diversity of the barcoded
813 phorids. Distance based mOTU delimitation was based on SpeciesIdentifier [59] while tree-
814 based mOTU delimitation was conducted using Poisson Tree Processes (PTP) model [61]. The
815 number of species was estimated using three different thresholds (2%, 3%, 4%). To understand
816 if these thresholds are not misleading for Phoridae, we examined the publicly available data in
817 GenBank for this family. We downloaded 79,506 phorid COI sequences to from NCBI using the
818 following search terms: txid36164[Organism] AND (COI[Gene Name] OR Cox1[Gene Name]
819 OR COXI[Gene Name] OR “cytochrome oxidase subunit 1”[Gene Name] OR “cytochrome c
820 oxidase subunit 1”[Gene Name] OR “cytochrome oxidase subunit I”[Gene Name]). The data
821 were filtered to exclude unidentified barcode records (containing sp. or identified as Phoridae

822 BOLD) and sequences that had <500 bp overlap with the 658 bp COI 5' barcoding region. Four
823 additional sequences were excluded as they resulted in a frameshift in the sequence alignment
824 conducted using MAFFT. The final alignment contained 12,072 DNA barcodes corresponding to
825 106 species, 74 of which had multiple barcodes. The barcodes corresponding to these 74
826 species were used to assess the distribution of pairwise intraspecific genetic distances. All
827 12,072 barcodes were clustered at various distance thresholds (1-10%) and the congruence
828 with morphology was assessed using match ratios. Congruence was highest for a 3% threshold
829 which was then also used to for estimating the species richness in the Ugandan sample of
830 phorids. The species richness estimation was carried out with EstimateS9 [62] using the
831 classical formula of Chao1 given that the coefficient of variation of the abundance or incidence
832 distribution was >0.5.

833 For tree based species delimitation, the PTP model [61] was applied on a maximum likelihood
834 phylogeny built using the aligned haplotypes of consolidated barcode dataset and the
835 GTRGAMMA model in RaXML v 8.4.2 [63]. Twenty independent searches were conducted to
836 obtain the best scoring phylogeny. PTP model was then applied on the resulting best scoring
837 ML phylogeny (mPTP --single --ML) [64].

838 **9. Morphological examination**

839 For morphological examination of the clustered specimens we used 100 randomly selected non-
840 singleton mOTUs delimited at 5% but also kept track of sub-clusters within the large mOTUs
841 that were splitting at 1-5%. This allowed for examination of closely related, but potentially
842 distinct, species. We were mostly interested in understanding if MinION barcodes were placing
843 specimens into mOTUs incorrectly and hence examined if the specimens were consistent
844 morphologically in each of these 5% clusters. The choice of 5% cluster may seem initially
845 inconsistent with the choice of 3% for mOTU delimitation for other analyses, but examination of
846 all specimens within 5% clusters allows for comparing multiple closely related 3% (or 1-5%)

847 mOTUs. For the strictest evaluation, this would often require genitalia preparations, but for
848 reasons of scope, this was here only carried out for one species. For this species we illustrate
849 how the haplotype network obtained with the median joining method in PopART (Fig. 7) [65]
850 guides the morphological examination of specimens for the new species, *Megaselia sepsioides*
851 sp. nov.. Specimens with the most dissimilar haplotypes were dissected in order to rule out the
852 presence of multiple closely related species. Differences in setation were observed between the
853 two distant haplotypes (UGC0012899 and UGC0012244) and the main cluster (UGC0003003,
854 UGC0005864, UGC0005996, UGC0012568, UGC0012937, and UGC0012971) and are
855 illustrated in Fig. 6. Specimen examination was done with a Leica m80 and Leica M205 C
856 stereo microscopes and the images were obtained with a Dun Inc. Microscope
857 Macrophotography system (Canon 7D chassis with 10X Mitutoyo lens). Photography stacking
858 was done with Zerene stacker. Specimens were cleared with clove oil and mounted on slides in
859 Canada balsam following the protocol of Disney [66]. The type series is housed in the Lee Kong
860 Chian Natural History Museum, Singapore.

861

862 **List of abbreviations:**

863 mOTU: molecular Operational Taxonomic Units

864 NGS: Next Generation Sequencing

865 NuMTs: Nuclear mitochondrial DNA sequences

866 BIN: Barcode Index Number

867 PTP: Poisson Tree Processes

868 MSA: Multiple Sequence Alignment

869

870 **DECLARATIONS**

871 **Ethics approval and consent to participation:**

872 The specimens were collected with valid permits (see acknowledgements).

873 **Consent for publication:** Not applicable

874 **Availability of data and materials**

875 Source code:

876 - Project name: *miniBarcoder*
877 - Project home page: https://github.com/asrivathsan/miniBarcoder [67]
878 - Operating system(s): Linux, MacOSX
879 - Programming language: Python
880 - Other requirements: MAFFT BARCODE: MAFFT, glsearch36, RACON BARCODE:
881 GraphMap, Racon, and amino acid correction: BioPython, BLAST and MAFFT.
882 - License: GNU GPL
883 - New scripts included: mb_parallel_consensus.py mb_parallel_demultiplex.py,
884 repool_by_plate.py
885 - Updated scripts: consolidate.py, aacorrection.py

886 Others

887 Nanopore raw reads are available in NCBI SRA, project PRJNA563237 (SRR10054347-
888 SRR10054350) [68] and the consolidated barcodes are available in FigShare [69] and
889 GenBank (Accession Nos. MN403320-MN410421). The Additional File 6 contains the
890 information for demultiplexing the data.

891 **Competing Interests**: The authors declare that they have no competing interests.

892 **Funding:** We would like to acknowledge support from the following grants: MOE grant for
893 biodiversity discovery (R-154-000-A22-112), NUS SEABIG grant (R-154-000-648-646 and R-
894 154-000-648-733), and institutional research funding (IUT21-1) of the Estonian Ministry of
895 Education and Research for O.K..

896 **Author's Contributions:** R.M. and A.S. conceived the workflow and the analytical approach.
897 O.K. conducted/organized the sampling and Diptera sorting and commented on the manuscript.
898 Molecular work was conducted by J.P., W.T.L., S.N.K., E.H. and A.S. Pipeline development and
899 data analyses was conducted by A.S. Morphological examination, and species description was
900 conducted by E.H. Figures were prepared by E.H., S.N.K., A.S. Manuscript was written by R.M.,
901 A.S. and E.H..

902 **Acknowledgements:** The material in Kibale National Park in Uganda was collected and
903 transferred in accordance with approvals from the Uganda Wildlife Authority (UWA/FOD/33/02)
904 and Uganda National Council for Science and Technology (NS 290/ September 8, 2011),
905 respectively. Yuchen Ang is thanked for his help photographing the new species and for his
906 suggestion of sepsioides as the specific epithet. Henry Disney and Brian Brown are thanked for
907 their consultation on the new species of *Megaselia*. We thank Arina Adom for help in curating
908 the Illumina barcodes and Sabrina Tang for help with photography.

909

910

911 **REFERENCES**

912 1. May RM: **Why worry about how many species and their loss?** *PLoS Biology* 2011,
913 **9**(8):e1001130.
914 2. Wilson EO: **Biodiversity research requires more boots on the ground**. *Nat Ecol Evol*
915 2017, **1**(11):1590-1591.

916 3. Riedel A, Sagata K, Suhardjono YR, Tänzler R, Balke M: **Integrative taxonomy on the**
917 **fast track - towards more sustainability in biodiversity research**. *Frontiers in*
918 *Zoology* 2013, **10**:15.
919 4. Wang WY, Srivathsan A, Foo M, Yamane SK, Meier R: **Sorting specimen-rich**
920 **invertebrate samples with cost-effective NGS barcodes: Validating a reverse**
921 **workflow for specimen processing.** *Molecular Ecology Resources* 2018, **18**(3):490-
922 501.
923 5. Krell F-T: **Parataxonomy vs. taxonomy in biodiversity studies – pitfalls and**
924 **applicability of 'morphospecies' sorting**. *Biodiversity and Conservation* 2004,
925 **13**(4):795-812.
926 6. Tänzler R, Sagata K, Surbakti S, Balke M, Riedel A: **DNA barcoding for community**
927 **ecology- How to tackle a hyperdiverse, mostly undescribed Melanesian fauna**.
928 *PLoS One* 2012, **7**(1):e28832.
929 7. Yeo D, Puniamoorthy J, Ngiam RWJ, Meier R: **Towards holomorphology in**
930 **entomology: rapid and cost-effective adult–larva matching using NGS barcodes**.
931 *Systematic Entomology* 2018, **43**(4):678-691.
932 8. Meier R, Wong W, Srivathsan A, Foo M: **$1 DNA barcodes for reconstructing**
933 **complex phenomes and finding rare species in specimen-rich samples**. *Cladistics*
934 2016, **32**(1):100-110.
935 9. Wong WH, Tay YC, Puniamoorthy J, Balke M, Cranston PS, Meier R: **'Direct PCR'**
936 **optimization yields a rapid, cost-effective, nondestructive and efficient method for**
937 **obtaining DNA barcodes without DNA extraction**. *Molecular Ecology Resources*
938 2014, **14**(6):1271-1280.
939 10. Hebert PDN, Braukmann TWA, Prosser SWJ, Ratnasingham S, deWaard JR, Ivanova
940 NV, Janzen DH, Hallwachs W, Naik S, Sones JE *et al*: **A Sequel to Sanger: amplicon**
941 **sequencing that scales**. *BMC Genomics* 2018, **19**:219.

942 11. Shokralla S, Porter TM, Gibson JF, Dobosz R, Janzen DH, Hallwachs W, Golding B,
943 Hajibabaei M: **Massively parallel multiplex DNA sequencing for specimen**
944 **identification using an Illumina MiSeq platform**. *Scientific Reports* 2015, **5**:9687.
945 12. Creedy TJ, Norman H, Tang CQ, Chim KQ, Andujar C, Arribas P, O'Connor R, Carvell
946 C, Notton DG, Vogler AP: **A validated workflow for rapid taxonomic assignment and**
947 **monitoring of a national fauna of bees (Apiformes) using high throughput DNA**
948 **barcoding.** *Molecular Ecology Resources* 2019, DOI:10.1111/1755-0998.13056.
949 13. Krehenwinkel H, Kennedy SR, Rueda A, Lam A, Gillespie RG: **Scaling up DNA**
950 **barcoding – Primer sets for simple and cost efficient arthropod systematics by**
951 **multiplex PCR and Illumina amplicon sequencing.** *Meth Ecol Evol,* 2018,
952 9(11):2181–2193.
953 14. Srivathsan A*, Baloğlu B*, Wang W, Tan WX, Bertrand D, Ng AHQ, Boey EJH, Koh JJY,
954 Nagarajan N, Meier R: **A MinION™-based pipeline for fast and cost-effective DNA**
955 **barcoding**. *Molecular Ecology Resources* 2018, **18**(5):1035-1049.
956 15. Pomerantz A, Penafiel N, Arteaga A, Bustamante L, Pichardo F, Coloma LA, Barrio-
957 Amoros CL, Salazar-Valenzuela D, Prost S: **Real-time DNA barcoding in a rainforest**
958 **using nanopore sequencing: opportunities for rapid biodiversity assessments and**
959 **local capacity building.** *GigaScience* 2018, **7**(4):giy033.
960 16. Blanco M, Greene LK, Williams RC, Andrianandrasana L, Yoder AD, Larsen PA: **Next-**
961 **generation in situ conservation and educational outreach in Madagascar using a**
962 **mobile genetics lab**. *BioRxiv* 2019, DOI:10.1101/650614.
963 17. Menegon M, Cantaloni C, Rodriguez-Prieto A, Centomo C, Abdelfattah A, Rossato M,
964 Bernardi M, Xumerle L, Loader S, Delledonne M: **On site DNA barcoding by nanopore**
965 **sequencing**. *PLoS One* 2017, **12**(10):e0184741.

966 18. Maestri S, Cosentino E, Paterno M, Freitag H, Garces JM, Marcolungo L, Alfano M,
967 Njunjic I, Schilthuizen M, Slik F *et al*: **A rapid and accurate MinION-based workflow**
968 **for tracking species biodiversity in the field**. *Genes* 2019, **10**(6):468.
969 19. Wick RR, Judd LM, Holt KE: **Performance of neural network basecalling tools for**
970 **Oxford Nanopore sequencing**. *Genome Biol* 2019, **20**:129.
971 20. Stork NE: **How many species of insects and other terrestrial arthropods are there**
972 **on Earth?** *Annu Rev Entomol* 2018, **63**:31-45.
973 21. Zhang ZQ: **Animal biodiversity: An introduction to higher-level classification and**
974 **taxnomic richness**, vol. 3148: Magnolia Press; 2011.
975 22. Farrell BD: **"Inordinate fondness" explained: Why are there so many beetles?**
976 *Science* 1998, **281**(5376):555-559.
977 23. Forbes AA, Bagley RK, Beer MA, Hippee AC, Widmayer HA: **Quantifying the**
978 **unquantifiable: why Hymenoptera – not Coleoptera – is the most speciose animal**
979 **order**. *BMC Ecology* 2018, **18**(21).
980 24. Ratnasingham S, Hebert PDN: **A DNA-based registry for all animal species: The**
981 **Barcode Index Number (BIN) system**. *PLoS One* 2013, **8**(7):e66213.
982 25. Hebert PD, Ratnasingham S, Zakharov EV, Telfer AC, Levesque-Beaudin V, Milton MA,
983 Pedersen S, Jannetta P, deWaard JR: **Counting animal species with DNA barcodes:**
984 **Canadian insects**. *Philos Trans R Soc Lond B Biol Sci* 2016, **371**(1702).
985 26. Borkent ART, Brown BV, Adler PH, Amorim DDS, Barber K, Bickel D, Boucher S,
986 Brooks SE, Burger J, Burington ZL *et al*: **Remarkable fly (Diptera) diversity in a patch**
987 **of Costa Rican cloud forest: Why inventory is a vital science**. *Zootaxa* 2018,
988 **4402**(1): 53-90.
989 27. Brown BV, Borkent A, Adler PH, De Souza Amorim D, Barber K, Bickel D, Boucher S,
990 Brooks SE, Burger J, Burington ZL *et al*: **Comprehensive inventory of true flies**
991 **(Diptera) at a tropical site**. *Communications Biology* 2018, **1**(21):8.

992 28. **Phorid Catalog** [http://phorid.net/pcat/]
993 29. Brown BV, Hartop EA: **Big data from tiny flies: patterns revealed from over 42,000**
994 **phorid flies (Insecta: Diptera: Phoridae) collected over one year in Los Angeles,**
995 **California, USA**. *Urban Ecosystems* 2016, **20**(3): 521-534.
996 30. Marshall SA: **Flies: The Natural History and Diversity of Diptera**. Buffalo, New York:
997 Firefly Books; 2012.
998 31. Vaser R, Sović I, Nagarajan N, Šikić M: **Fast and accurate de novo genome assembly**
999 **from long uncorrected reads**. *Genome research* 2017, **27**(5):737-746.
1000 32. Kwong S, Srivathsan A, Vaidya G, Meier R: **Is the COI barcoding gene involved in**
1001 **speciation through intergenomic conflict?.** *Molecular Phylogenetics and Evolution*
1002 2012, **62**(3):1009.-1012
1003 33. Hartop EA, Brown BV: **The tip of the iceberg: a distinctive new spotted-wing**
1004 ***Megaselia* species (Diptera: Phoridae) from a tropical cloud forest survey and a**
1005 **new, streamlined method for *Megaselia* descriptions**. *Biodiversity Data Journal*
1006 2014, **2**:e4093.
1007 34. Hartop EA, Brown BV, Disney RHL: **Opportunity in our ignorance: urban biodiversity**
1008 **study reveals 30 new species and one new Nearctic record for *Megaselia* (Diptera:**
1009 **Phoridae) in Los Angeles (California, USA)**. *Zootaxa* 2015, **3941**:451-484.
1010 35. Hartop EA, Brown BV, Disney RHL: **Flies from L.A., The Sequel: Twelve further new**
1011 **species of *Megaselia* (Diptera: Phoridae) from the BioSCAN Project in Los**
1012 **Angeles (California, USA)**. In: *Biodiversity Data Journal.* vol. 4; 2016: e7756.
1013 36. Riedel A, Sagata K, Surbakti S, Rene T, Michael B: **One hundred and one new**
1014 **species of Trigonopterus weevils from New Guinea**. *Zookeys* 2013(280):1-150.
1015 37. Meier R, Zhang G, Ali F: **The use of mean instead of smallest interspecific**
1016 **distances exaggerates the size of the "barcoding gap" and leads to**
1017 **misidentification**. *Systematic Biology* 2008, **57**(5):809-813.

1018 38. Erwin TL: **Tropical forests: Their richness in Coleoptera and other arthropod**
1019 **species**. *The Coleopterists Bulletin* 1982, **36**(1):74-75.
1020 39. Longino JT, Coddington J, Colwell RK: **The ant fauna of a tropical rain forest:**
1021 **estimating species richness three different ways**. *Ecology* 2002, **83**:689-702.
1022 40. Butcher BA, Smith MA, Sharkey MJ, Quicke DLJ: **A turbo-taxonomic study of Thai**
1023 **Aleiodes (Aleiodes) and Aleiodes (Arcaleiodes) (Hymenoptera: Braconidae:**
1024 **Rogadinae) based largely on COI barcoded specimens, with rapid descriptions of**
1025 **179 new species.** *Zootaxa* 2012, **3457**(1):1-232.
1026 41. Riedel A, Narakusumo RP: **One hundred and three new species of Trigonopterus**
1027 **weevils from Sulawesi**. *ZooKeys* 2019, **828**:1-153.
1028 42. Riedel A, Tänzler R, Balke M, Rahmadi C, Suhardjono YR: **Ninety-eight new species**
1029 **of Trigonopterus weevils from Sundaland and the Lesser Sunda Islands**. *ZooKeys*
1030 2014, **467**:1-162.
1031 43. ONT Store: https://store.nanoporetech.com/kits-250/1d-sequencing-kit.html
1032 44. Townes H: **A light-weight Malaise trap**. *Entomological News* 1972, **83**:239-247.
1033 45. Howard PC: **Nature conservation in Uganda's tropical forest reserves**. *The IUCN*
1034 *Tropical Forest Programme* 1991.
1035 46. Chapman CA, Chapman LJ: **Forest regeneration in logged and unlogged forests of**
1036 **Kibale National Park, Uganda**. *Biotropica* 1997, **29**:396-412.
1037 47. Kurina O: **Description of four new species of *Zygomyia* Winnertz from Ethiopia and**
1038 **Uganda (Diptera: Mycetophilidae)**. *African Invertebrates* 2012, **53**(1):205-220.
1039 48. Folmer O, Black M, Hoeh W, Lutz R, Vrijenhoek R: **DNA primers for amplification of**
1040 **mitochondrial cytochrome c oxidase I from diverse metazoan invertebrates**.
1041 *Molecular Marina Biology and Technology* 1994, **3**(5):294-299.

1042 49. Comai L, Howell T: **Barcode Generator**.
1043 *http://comailabgenomecenterucdavisedu/indexphp/Barcode_generator.* 2012.
1044 50. Krehenwinkel H, Pomerantz A, Henderson JB, Kennedy SR, Lim JY, Swamy V,
1045 Shoobridge JD, Graham N, Patel NH, Gillespie RG *et al*: **Nanopore sequencing of**
1046 **long ribosomal DNA amplicons enables portable and simple biodiversity**
1047 **assessments with high phylogenetic resolution across broad taxonomic scale**.
1048 *GigaScience* 2019, 85(5):giz006.
1049 51. Katoh K, Standley DM: **MAFFT multiple sequence alignment software version 7:**
1050 **improvements in performance and usability.** *Molecular Biology and Evolution* 2013,
1051 **30**(4):772-780.
1052 52. Sović I, Šikić M, Wilm A, Fenlon SN, Chen S, Nagarajan N: Fast and sensitive mapping
1053 of nanopore sequencing reads with GraphMap. *Nature Communications* 2016, **7**:11307.
1054 53. Leray M, Yang JY, Meyer CP, Mills SC, Agudelo N, Ranwez V, Boehm JT, Machida RJ:
1055 **A new versatile primer set targeting a short fragment of the mitochondrial COI**
1056 **region for metabarcoding metazoan diversity: application for characterizing coral**
1057 **reef fish gut contents**. *Frontiers in Zoology* 2013, **10**:34.
1058 54. Geller J, Meyer C, Parker M, Hawk H: **Redesign of PCR primers for mitochondrial**
1059 **cytochrome c oxidase subunit I for marine invertebrates and application in all-taxa**
1060 **biotic surveys**. *Molecular Ecology Resources* 2013, **13**(5):851-861.
1061 55. Yeo D, Srivathsan A, Meier R: **Longer is not always better: Optimizing barcode**
1062 **length for large-scale species discovery and identification**. *bioRxiv* 2019:
1063 DOI:10.1101/594952.
1064 56. Zhang J, Kobert K, Flouri T, Stamatakis A: **PEAR: a fast and accurate Illumina Paired-**
1065 **End reAd mergeR.** *Bioinformatics* 2014, **30**(5):614-620.

1066 57. Srivathsan A, Sha JC, Vogler AP, Meier R: **Comparing the effectiveness of**
1067 **metagenomics and metabarcoding for diet analysis of a leaf-feeding monkey**
1068 **(*Pygathrix nemaeus*)**. *Molecular Ecology Resources* 2015, **15**(2):250-261.
1069 58. Kurtz S, Phillippy A, Delcher AL, Smoot M, Shumway M, Antonescu C, Salzberg SL:
1070 **Versatile and open software for comparing large genomes**. *Genome Biol* 2004,
1071 **5**(2):R12.
1072 59. Meier R, Shiyang K, Vaidya G, Ng PKL: **DNA Barcoding and Taxonomy in Diptera: A**
1073 **Tale of High Intraspecific Variability and Low Identification Success**. *Systematic*
1074 *Biology* 2006, **55**(5):715–728.
1075 60. Ahrens D, Fujisawa T, Krammer HJ, Eberle J, Fabrizi S, Vogler AP: **Rarity and**
1076 **Incomplete Sampling in DNA-based Species Delimitatio**. *Systematic Biology* 2016,
1077 **65**(3):478-494.
1078 61. Zhang J, Kapli P, Pavlidis P, Stamatakis A: **A general species delimitation method**
1079 **with applications to phylogenetic placements**. *Bioinformatics* 2013, **29**(22):2869-
1080 2876.
1081 62. Colwell RK: **EstimateS: Statistical estimation of species richness and shared**
1082 **species from samples. Version 9 and earlier. User's Guide and application.** 2013.
1083 63. Stamatakis A: **RAxML version 8: a tool for phylogenetic analysis and post-analysis**
1084 **of large phylogenies**. *Bioinformatics* 2014, **30**(9):1312-1313.
1085 64. Kapli P, Lutteropp S, Zhang J, Kobert K, Pavlidis P, Stamatakis A, Flouri T: **Multi-rate**
1086 **Poisson tree processes for single-locus species delimitation under maximum**
1087 **likelihood and Markov chain Monte Carlo.** *Bioinformatics* 2017, **33**(11):1630-1638.
1088 65. Leigh JW, Bryant D: **PopART: Full-feature software for haplotype network**
1089 **construction.** *Methods Ecol Evol* 2015, **6**(9):1110-1116.
1090 66. Disney RHL: **Scuttle flies (Diptera: Phoridae) Part II: the genus *Megaselia***. *Fauna of*
1091 *Arabia* 2009, **24**:249-357.

1092 67. Srivathsan A: **miniBarcoder**. Github: https://github.com/asrivathsan/miniBarcoder.

1093 68. Srivathsan A, Hartop E, Puniamoorthy J, Lee WT, Kutty SN, Kurina O, Meier R: **1D**
1094 **MinION sequencing for large-scale species discovery: 7000 scuttle flies (Diptera:**
1095 **Phoridae) from one site in Kibale National Park (Uganda) revealed to belong to**
1096 **>650 species.** NCBI SRA: https://www.ncbi.nlm.nih.gov/bioproject/PRJNA563237.

1097 69. Srivathsan A, Hartop E, Lee, WT, Puniamoorthy J, Kutty SN, Meier R (2019):
1098 **Consolidated barcode set associated with the study: Rapid, large-scale species**
1099 **discovery in hyperdiverse taxa using 1D MinION sequencing1D**. figshare, 2019.
1100 Dataset: https://doi.org/10.6084/m9.figshare.9932720.

1101

1102

1103 **Figure Legends**

1104 **Figure 1**: Flowchart for generating MinION barcodes from experimental set-up to final barcodes.
1105 The novel steps introduced in this study are highlighted in green and the scripts available in
1106 *miniBarcoder* for analyses are further indicated.

1107 **Figure 2**: Effect of re-pooling on coverage of barcodes for both sets of specimens. Barcodes
1108 with coverage <50X were re-pooled and hence the coverage of these barcodes increases.

1109 **Figure 3**: Ambiguities in MAFFT+AA (Purple), RACON+AA (Yellow) and Consolidated barcodes
1110 (Green) with varying namino parameters (1,2 and 3). One outlier value for Racon+3AA barcode
1111 was excluded from the plot. The plot shows that the consolidated barcodes have few
1112 ambiguities remaining.

1113 **Figure 4**: The Malaise trap that revealed the estimated >1000 mOTUs as shown by the species
1114 richness estimation curve. Green: Chao1 Mean, Pink: S (Mean), Orange: Singleton Mean,
1115 Purple: Doubleton mean.

1116 **Figure 5**: Lateral habitus (a) and diagnostic features of *Megaselia sepsioides* spec. nov. (a,
1117 inset) terminalia, (b) posterior view of foreleg, (c) anterior view of midleg (d,e) anterior and
1118 postero-dorsal views of hindleg, (e) dorsal view of thorax and abdomen.
1119 **Figure 6**: Haplotype variation of *Megaselia sepsioides* spec. nov. (a) UGC0005996, (b)
1120 UGC0012244, (c) UGC0012899. UGC numbers refer to specimen IDs.
1121 **Figure 7**: Haplotype network for *Megaselia sepsioides* spec. nov. UGC numbers refer to
1122 specimen IDs.
1123
1124 **ADDITIONAL FILES**
1125 Additional File 1.docx: Fig S1: Pairwise edit distances between tags. Fig S2 and S3: Analyses of
1126 GenBank phorid data
1127 Additional File 2.xlsx: Tag sequences used in this study
1128 Additional File 3.xlsx: Details on incongruent clusters
1129 Additional File 4.xlsx: Analyses of paralogs/contaminations
1130 Additional File 5.xlsx: Details on specimens with >3% divergence from Illumina barcodes for
1131 final consolidated barcode sets
1132 Additional File 6.xlsx: Demultiplexing information for the two sample sets

Table 1: Number of reads and barcodes generated via MinION sequencing.

	Set 1: Two flowcells	**Set 2: One flowcell**	**Combined (set 1 & 2)***
# Specimens	4,275	4,519	8,699
Resequencing (re-pooled)	2,172	2,211	
# reads/# reads >600 bp	7,035,075/3,703,712	7,179,121/2,652,657	NA
Initial sequencing (all)	3,069,048/1,942,212	4,853,363/2,250,591	
Resequencing (re-pooled)	3,966,027/1,761,500	2,325,758/402,066	
# demultiplexed reads	898,979 (24.3%)	647,152 (24.4%)	
Initial sequencing (all)	562,434 (29%)	561,383 (24.9%)	
Resequencing (re-pooled	336,545 (19%)	85,769 (21.3%)	
Combined results of original and resequencing runs			
# specimens with >=5X coverage	4,227 (98.9%)	4,287 (94.9%)	8,428 (96.9%)
# MAFFT barcodes <1% N's	3,797 (88.8%)	3,476 (76.9%)	7,221 (83%)
# MAFFT + AA barcodes	3,771 (88.2%)	3,459 (76.5%)	7,178 (82.5%)
# RACON barcodes	3,797 (88.8%)	3,476 (76.9%)	7,221 (83%)
# RACON +AA barcodes	3,788 (88.6%)	3,461 (76.6%)	7,194 (82.7%)
# Consolidated barcodes	3,762 (88%)	3,446 (76.3%)	7,155 (82.3%)
# Consolidated barcodes (non-phorids removed)	3,727 (87.2%)	3,426 (75.8%)	7,059 (81.1%)
# mOTUS (2/3/4%)			**705/663/613**

* one plate was accidentally sequenced in both runs, duplicates removed for combined set.

Table 2. Accuracy of MinION as assessed by Illumina barcodes. The MinION barcodes were trimmed to the 313 bp that were sequenced using Illumina. The overall optimal strategy is “Consolidated (namino=2)”. Optimal congruence values are highlighted in bold.

Dataset	**# compared with Illumina/ # 3% mOTUs**	**Accuracy Mean (stdev)**	**%Ns**	**# barcodes with errors/# >3% errors**	**mOTU richness deviation between MinION and Illumina barcodes**		
					2%	**3%**	**4%**
MAFFT	6,291/641	99.6136 (0.37)	0.18 (0.2)	4,473/30	-3 (-0.44%)	**-2 (-0.31%)**	-11 (-1.85%)
RACON	6,291/645	99.5097 (0.48)	<0.001 (0.01)	4,494/36	12 (1.72%)	**2 (0.31%)**	**-3 (-0.5%)**
MAFFT + AA (namino=1)	6,269/635	99.9689 (0.19)	1.19 (0.84)	273/27	-6 (-0.89%)	-6 (-0.94%)	-6 (-1.02%)
MAFFT + AA (namino=2)	6,269/635	99.9802 (0.15)	1.28 (0.92)	216/28	-8 (-1.19%)	-6 (-0.94%)	-14 (-2.37%)
MAFFT + AA (namino=3)	6,269/633	99.9685 (0.18)	1.25 (0.91)	310/27	-8 (-1.19%)	-8 (-1.26%)	-17 (-2.9%)
RACON + AA (namino=1)	6,273/639	99.9636 (0.19)	0.48 (0.47)	392/26	-4 (-0.59%)	-4 (-0.63%)	-13 (-2.19%)
RACON + AA (namino=2)	6,273/635	99.9736 (0.16)	0.55 (0.55)	288/26	-5 (-0.74%)	-8 (-1.26%)	-14 (-2.36%)
RACON + AA (namino=3)	6,273/636	99.9684 (0.17)	0.57 (0.6)	345/28	**-1 (-0.15%)**	-7 (-1.1%)	-13 (-2.19%)
Consolidated (namino=1)	6,229/639	99.9849 (0.12)	0.41 (0.44)	191/26	-2 (-0.29%)	**-2 (-0.31%)**	**-3 (-0.5%)**
Consolidated (namino=2)	6,251/638	**99.9859 (0.11)**	**0.46 (0.5)**	**184/25**	-2 (-0.29%)	-3 (-0.47%)	-5 (-0.83%)
Consolidated (namino=3)	6,245/639	99.9795 (0.12)	0.44 (0.49)	285/26	-4 (-0.59%)	**-2 (-0.31%)**	-4 (-0.67%)

Figure 1

WETLAB PROCEDURE

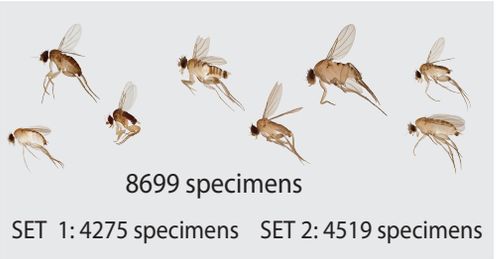

TAGGED PCRs

NEW:
- ▸96 new 13 bp tags
- ▸>=6bp substitution errors
- ▸>=3bp any type of error
- ▸<=2bp homopolymer

POOLING

Cleanup, normalization, pooling PCR products

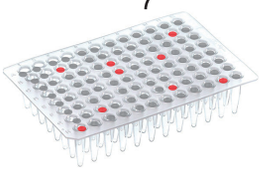

NEW: ▸Pick <=50X PCR products

SEQUENCING

NEW:
- ▸1D Library Preparation using SQK-LSK109
- ▸Basecalling using Guppy

COVERAGE ESTIMATION (repool_by_plate.py)

DEMULTIPLEXING (mb_parallel_demultiplex.py)

glsearch36 for primer idenfication
k-mer searches for tags

NEW:
- ▸ Homopolymer compression before k-mer searches
- ▸ Accounting for ligated products during glsearch
- ▸ Parallelization
- ▸ Reduced memory usage

BARCODE CALLING

MAFFT barcodes (mb_parallel_consensus.py)

Alignment of random 100 reads
Majority rule consensus

NEW: ▸ Parallelization

RACON barcodes

Mapping of reads using GraphMap to MAFFT barcodes

NEW:
- ▸ FASTA sequences for mapping
- ▸ max-error lowered to 0.15 for 1D reads

aacorrection .py

MAFFT + AA barcodes

RACON + AA barcodes

CONSOLIDATED barcodes (consolidate.py)

Alignment of MAFFT+AA and RACON+AA

Same nucleotide--> Accept nucleotide
One is "N" while other has a basecall--> Accept nucleotide

NEW:
- ▸ Mismatch--> "N"
- ▸ Increase gap opening penalty to 3
- ▸ indel within alignment of corrected barcodes--> reject barcode

SPECIES DELIMITATION

CONTAMINATION CHECK

mOTU CLUSTERING

NEW: ▸ Morphological examination

Figure 2

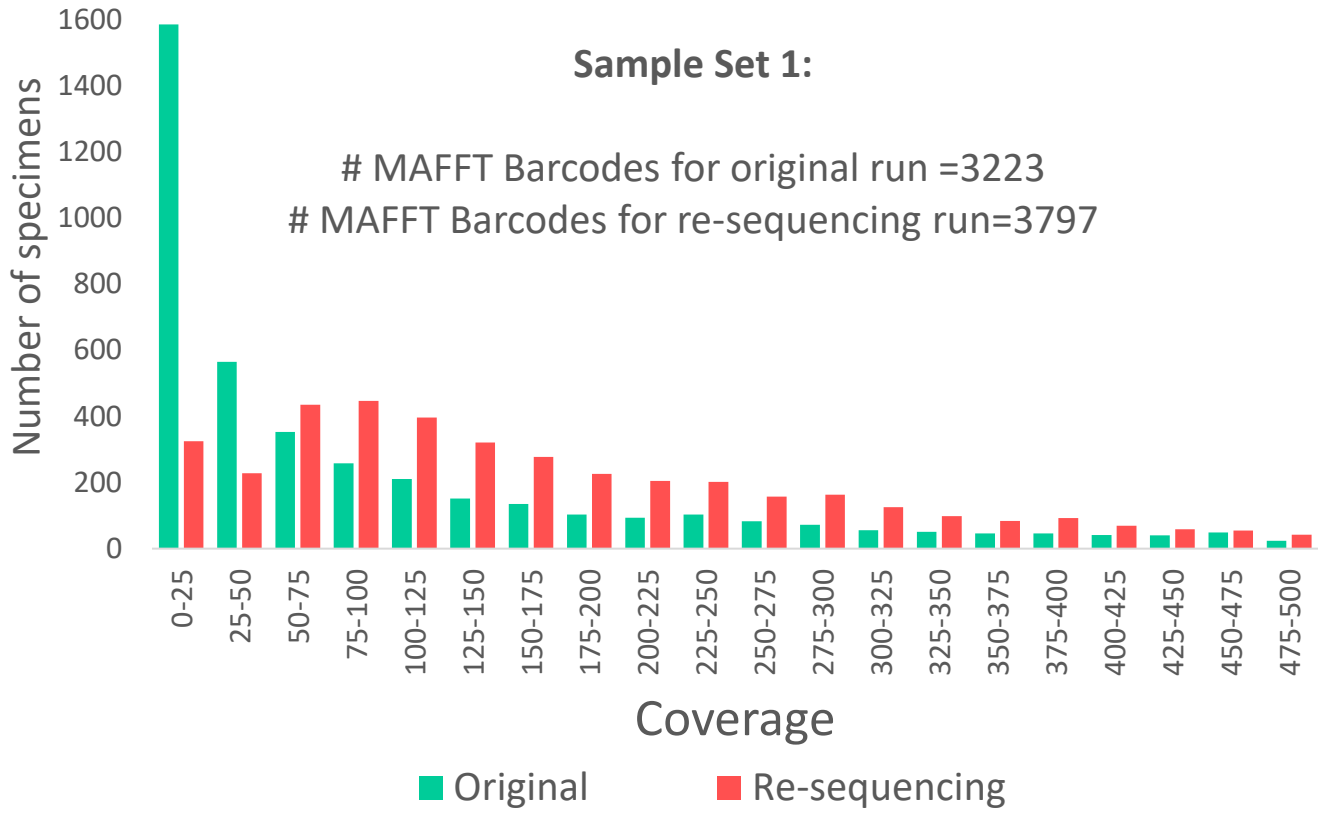
Sample Set 1:
MAFFT Barcodes for original run =3223
MAFFT Barcodes for re-sequencing run=3797
Number of specimens
1600
1400
1200
1000
800
600
400
200
0
0-25
25-50
50-75
75-100
100-125
125-150
150-175
175-200
200-225
225-250
250-275
275-300
300-325
325-350
350-375
375-400
400-425
425-450
450-475
475-500
Coverage
Original
Re-sequencing

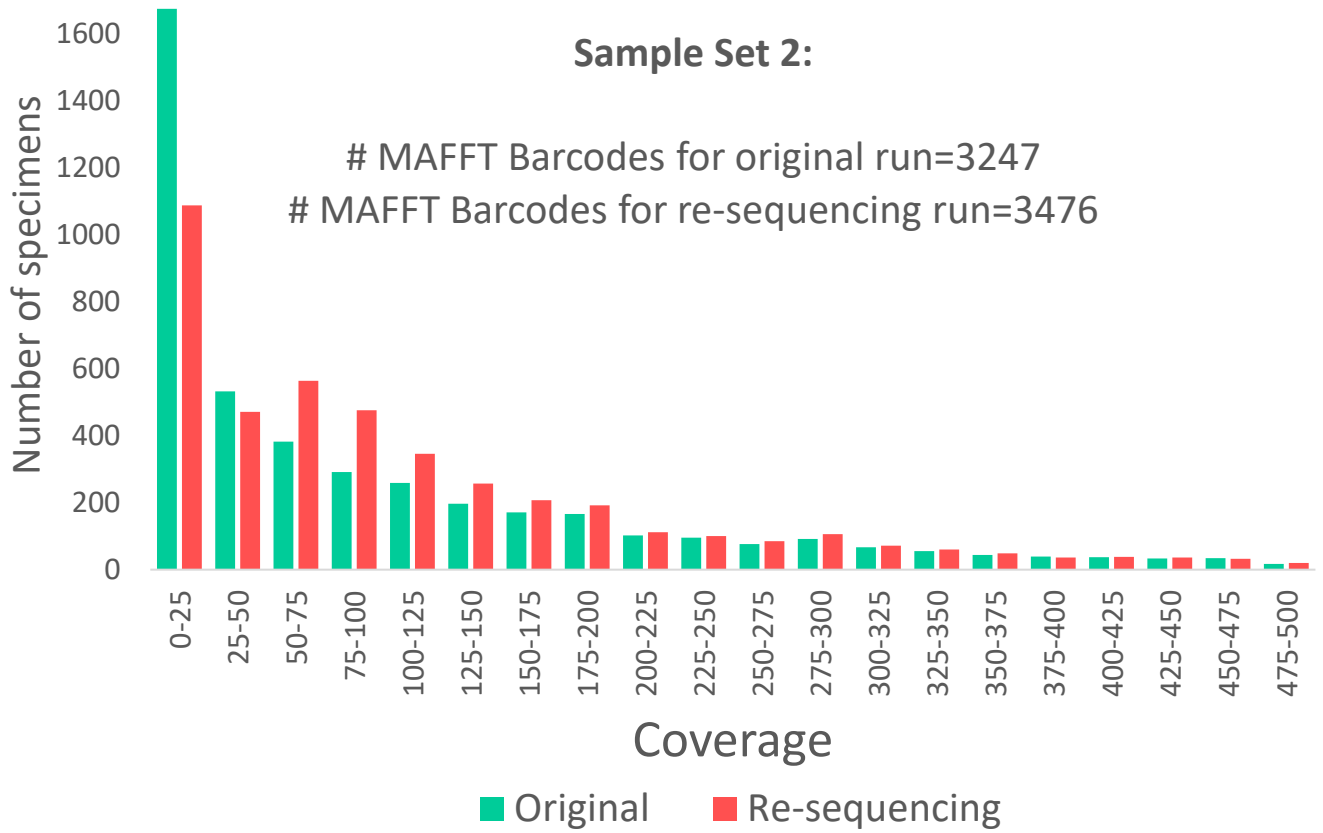
Sample Set 2:
MAFFT Barcodes for original run=3247
MAFFT Barcodes for re-sequencing run=3476
Number of specimens
1600
1400
1200
1000
800
600
400
200
0
0-25
25-50
50-75
75-100
100-125
125-150
150-175
175-200
200-225
225-250
250-275
275-300
300-325
325-350
350-375
375-400
400-425
425-450
450-475
475-500
Coverage
Original
Re-sequencing

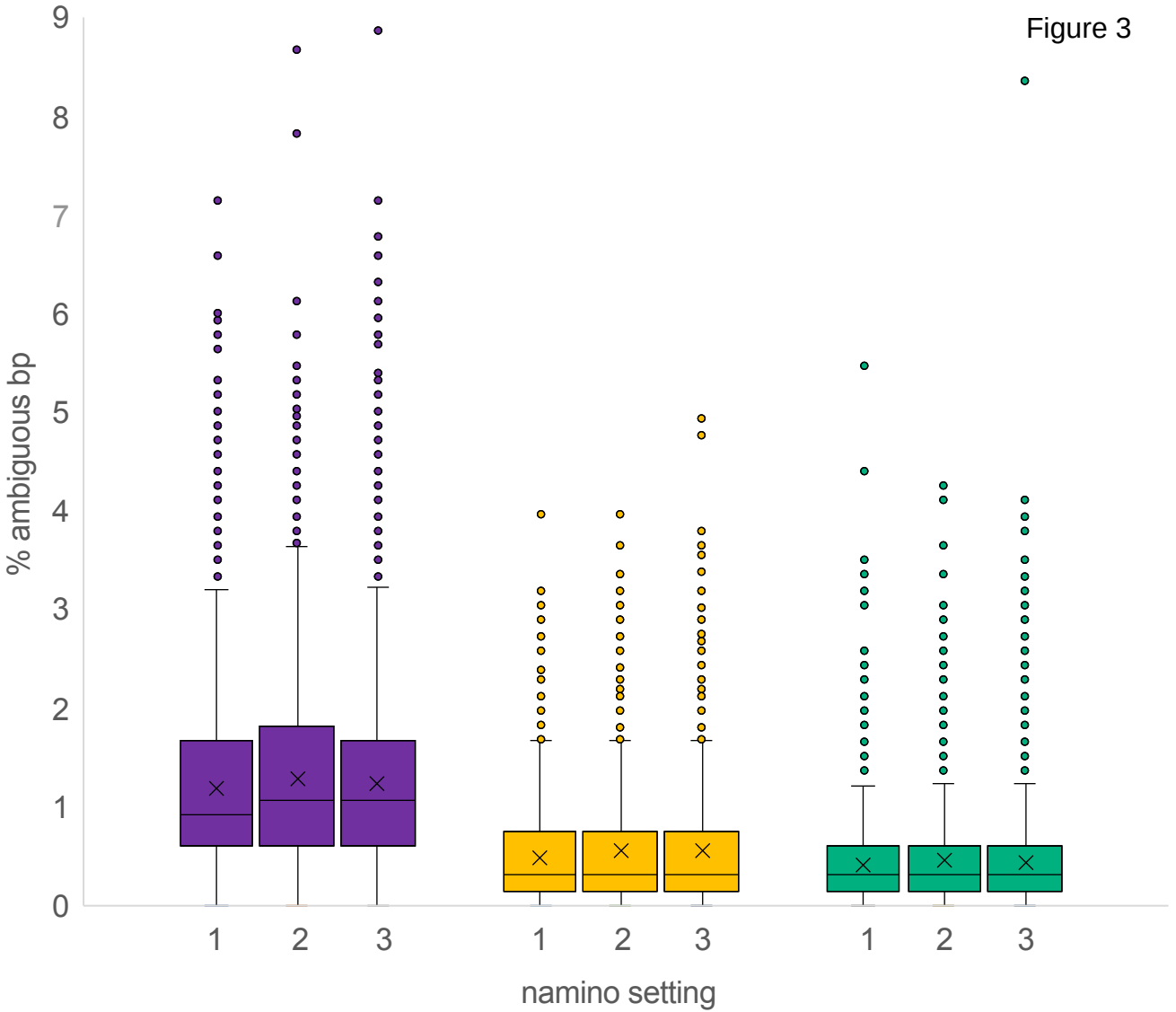
Figure 3
% ambiguous bp
0
1
2
3
4
5
6
7
8
9
1
2
3
1
2
3
1
2
3
namino setting

Figure 4

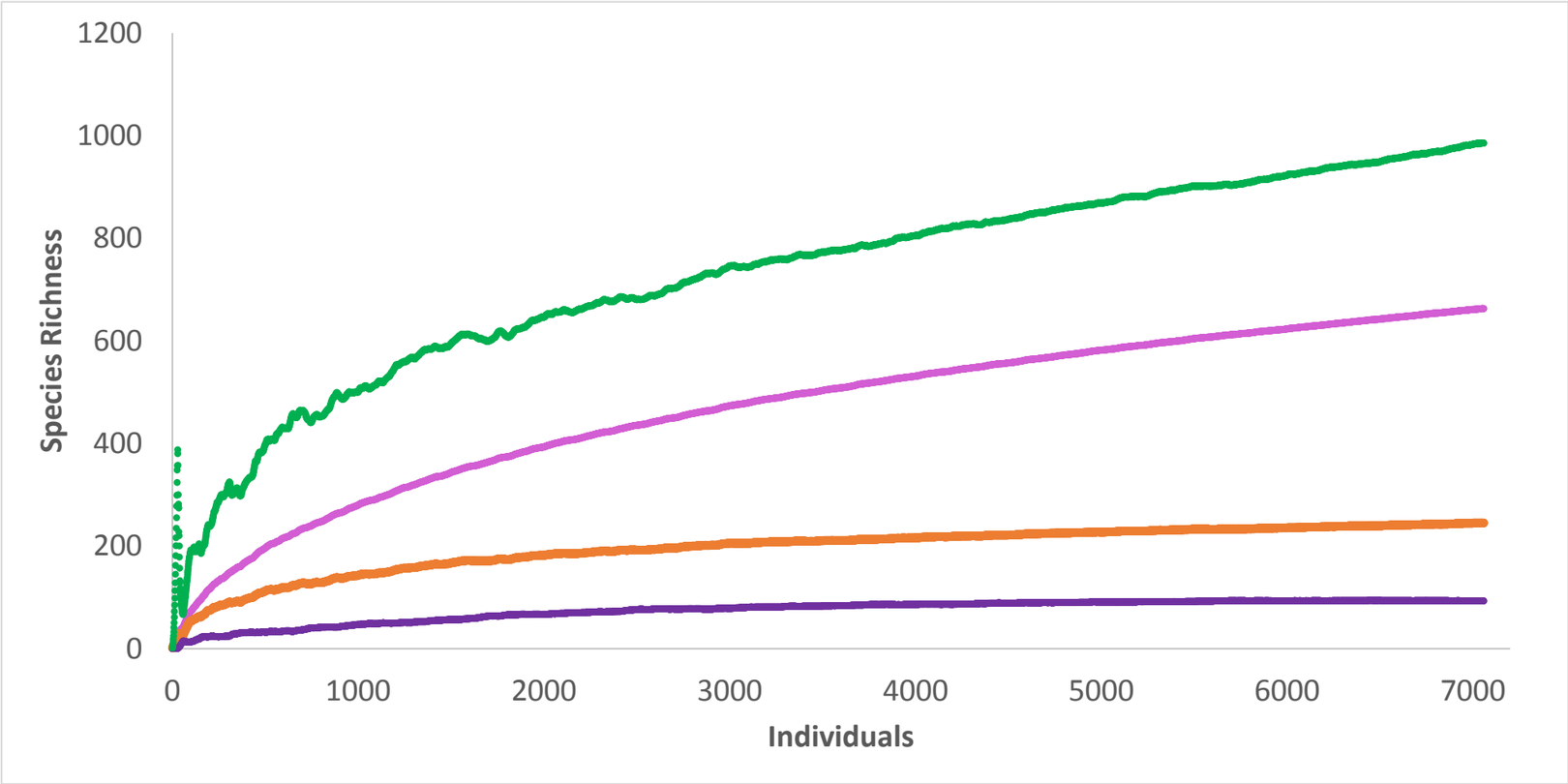
1200
1000
800
600
400
200
0
Species Richness
0
1000
2000
3000
4000
5000
6000
7000
Individuals

Figure 5

Figure 6

Figure 7

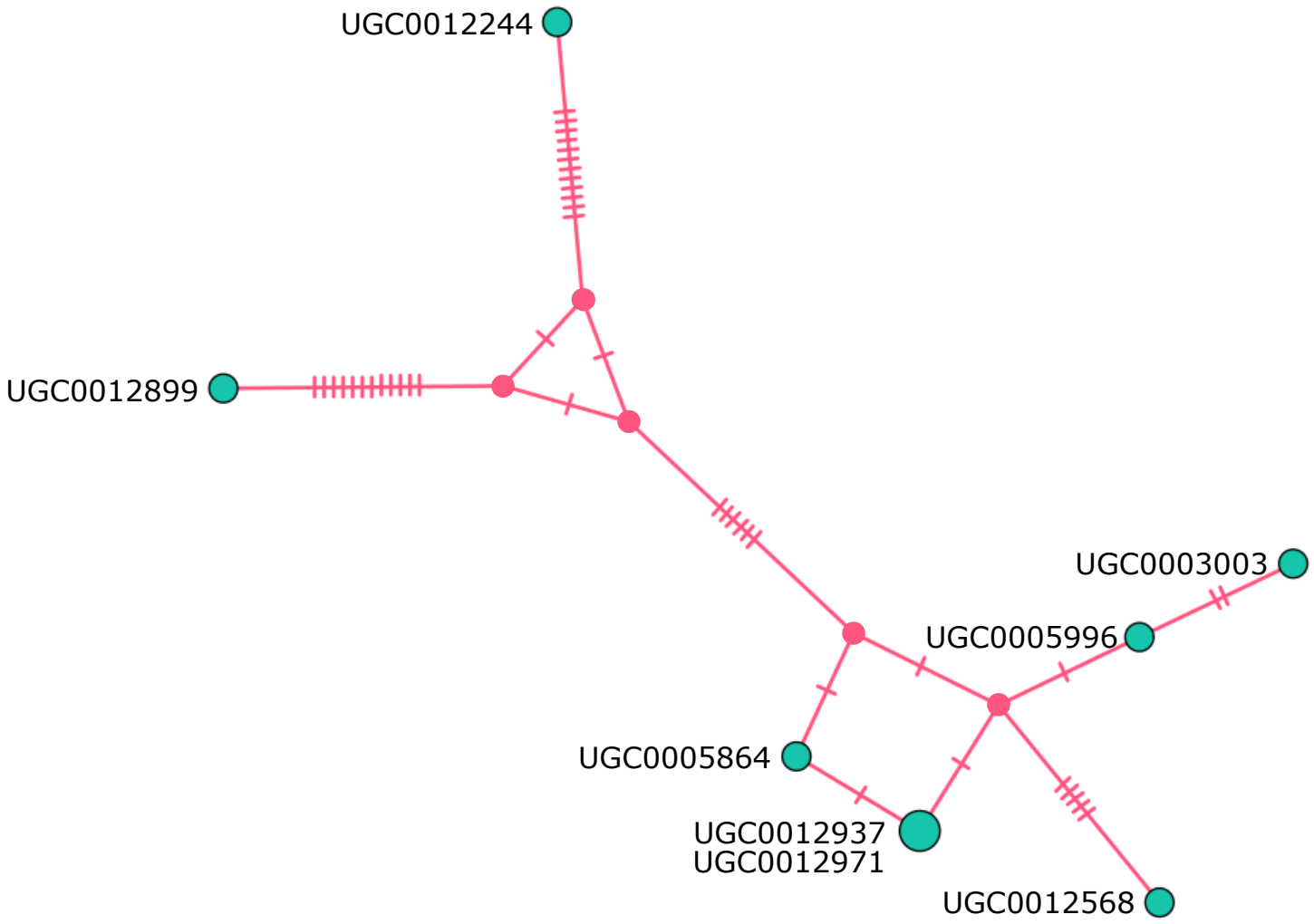
UGC0012244
UGC0012899
UGC0003003
UGC0005996
UGC0005864
UGC0012937
UGC0012971
UGC0012568